Digital Signal Processing 93 (2019) 1–21

Contents lists available at ScienceDirect

Digital Signal Processing

www.elsevier.com/locate/dsp

Primary signal detection algorithms for spectrum sensing at low SNR over fading channels in cognitive radio

Modar Shbat [a], Vyacheslav Tuzlukov [b,*]

[a] Networks and Telecommunications Engineering (IRTEL) Department, Polytechnic University of San Luis Potosi, Urbano Villalon #500, San Luis Potosi, Mexico
[b] Belarussian State Academy of Communications, Fransisco Scorina Street 8/2, Minsk 220114, Belarus

ARTICLE INFO

Article history:
Available online 6 August 2019

Keywords:
Cognitive radio (CR)
Spectrum sensing
Weighted generalized detector (WGD)
Generalized likelihood ratio test for GD (GLRT-GD)
Energy detector (ED)
Antenna array
Probability of false alarm
Probability of error
Optimal detection threshold

ABSTRACT

The generalized detector (GD) can be implemented at the low signal-to-noise ratio (SNR) in cognitive radio (CR) systems to improve the spectrum sensing performance under correlated antenna array elements. The weighted GD (WGD) and the generalized likelihood ratio test for GD (GLRT-GD) are proposed to be used for coarse spectrum sensing when the noise power is known and unknown, respectively. The GD optimal detection threshold is defined based on the minimum probability of error criterion for various fading channels, namely, the additive white Gaussian noise (AWGN), Nakagami-*m*, and Rayleigh fading channels. The performance of the proposed algorithms are compared with the spectrum sensing performance of the energy detector (ED), weighted ED (WED), maximum-minimum eigenvalue (MME) detector, generalized likelihood ratio test for ED (GLRT-ED), matched filter (MF), arithmetic to geometric mean (AGM) detector, scaled largest eigenvalue (SLE) detector, moment based detector (MBD), covariance based detector (CBD), and others. The simulation results demonstrate superiority in the spectrum sensing performance of the proposed algorithms in comparison with the above-mentioned detectors. For example, the GLRT-GD achieves the SNR gain equal to 1.2 dB, 4.0 dB, and 4.5 dB in comparison with GLRT-ED, MME, and GM detectors, respectively, at the probability of false alarm $P_{FA} = 0.1$. The WGD and GLRT-GD implementation allows us to achieve a considerable spectrum sensing performance improvement at small number of samples under the low SNR and the correlated antenna array elements.

1. Introduction

The spectrum scarcity problem under the rapid and huge growth of wireless sensor network service motivates many researchers to seek for various solutions. Approximately 70–80% band of the primary spectrum is already assigned and exclusively allocated to various types of wireless communications and sensor network technologies. New innovative techniques exploiting the available radio spectrum are required since only a part of the whole spectrum band is used at specified place and time [1]. Implementation of the cognitive radio (CR) systems allows us to alleviate the spectral congestion problem by opportunistic use of the frequency bands with the purpose to improve the efficiency of spectrum utilization. The CR principle encompasses several tasks such as the spectrum sensing, i.e., a detection of spectrum holes and interference avoidance, channel identification, i.e., the channel state estimation and capacity prediction, transmit power control, and dynamic spectrum management.

Spectrum sensing is needed to define the idle frequency bands, within the limits of which the entire CR operation is relied on. The radio spectrum awareness and existence of primary users (PUs) are obtained by performing the spectrum sensing at the secondary users (SUs) or secondary access nodes. As a result, the CR systems allow the SU to use the unutilized frequency bands without causing harmful interference to the PU. Many PU signal detection techniques can be applied in spectrum sensing [1], such as the energy detector (ED) [2,3], generalized likelihood ratio test (GLRT) detector [4], matched filter [5,6], cyclostationary detector [7,8], and eigenvalue-based detection algorithms [9]. There is no identification for a specific spectrum sensing technique in the related CR system standards (IEEE 802.22, IEEE 802.11K).

The cyclostationary detector can exploit the cyclostationary features embedded in the PU signal even at the low signal-to-noise ratio (SNR) [7,8]. In the MF case, a perfect knowledge about the PU signal parameters, namely, the bandwidth, operating frequency, modulation type and order, frame format, etc, is required to demodulate the received signal. The covariance-based detector

* Corresponding author.
E-mail addresses: modar.shbat@upslp.edu.mx (M. Shbat), slava.tuzlukov@mail.ru (V. Tuzlukov).

https://doi.org/10.1016/j.dsp.2019.07.016
1051-2004/

(CBD) exploits a difference in the statistical covariance of the received signal, generally, in practice it is estimated through the sample covariance matrix, and noise [10]. The decision statistics of the arithmetic to geometric mean (AGM) detector, maximum-minimum eigenvalue (MME) detector [11], energy to minimum eigenvalue (EME) detector [12], and scaled largest eigenvalue (SLE) detector [13] depend on the sample covariance matrix eigenvalues. The AGM test statistics is the ratio between the arithmetic mean and geometric mean of eigenvalues. The maximum and minimum eigenvalues of the PU signal covariance matrix are used to define the MME test statistics [11]. In the case of EME detector, the average power of received signal and the minimum eigenvalue of sample covariance matrix are defined to formulate the test statistics. MME and EME algorithms are called the blind detection methods because they use only the received signal samples to perform detection, similar to ED. The SLE detector [13] is based on GLRT with the final test statistics as a ratio of the largest eigenvalue to the sum of the sample covariance matrix eigenvalues. No a priori knowledge concerning the noise variance is required and, consequently, it is robust to the noise power uncertainty. The test statistics of the moment based detector (MBD) is the ratio of the fourth absolute moment to the square second absolute moment of practically relevant signal constellations [14]. The probability of detection formula for MBD differs according to the constellations, i.e., binary phase shift keying (BPSK), quadrature phase shift keying (QPSK), etc. For the max-min SNR based detector [15], the received signal is oversampled and the linear combining vector $\boldsymbol{\alpha}$ with the size L of oversampling factor is introduced assuming a known transmitter pulse shaping. The vector $\boldsymbol{\alpha}$ is optimized to have two components with different SNRs for the combined signal. The ratio of the signal energy corresponding to the maximum and minimum SNR is considered as the test statistics.

Useful ED sensing performance analysis is presented in [16]. The ED spectrum sensing performance and signal detection as a function of the average noise power fluctuations within the limits of short time interval are investigated in [17] and a new ED signal detection algorithm based on the dynamic detection threshold is discussed. Two stages spectrum sensing architecture combining the ED and feature detector is presented in [18]. This idea was proposed by IEEE 802.22 working group. The ED with two-steps threshold [19] and the weighted ED (WED) [20] achieve the significant spectrum sensing performance improvement in comparison with the conventional ED.

The idea to employ the generalized detector (GD) for the coarse spectrum sensing in CR systems has been triggered by the purpose to improve the spectrum sensing performance at the low SNR. The GD based on the generalized approach to signal processing (GASP) in noise [21–23] represents a combination of the correlation detector and ED. A great difference between the GD and conventional ED is a presence of additional linear system, for example, the band pass filter, at the GD input. This filter can be considered as the source of reference noise, which does not contain the PU signal. The GD log-likelihood ratio test (log-LFT), based on which we can make a decision about the PU signal presence or absence in the process incoming at the SU input, demonstrates a definition of the jointly sufficient statistics of the mean and variance at the GD output and does not require any information about the PU signal and its parameters [21], [22, Chapter 3]. Note, that the conventional correlation detector makes a decision about the PU signal presence or absence in the incoming process based on a definition of the log-LRT mean only. The conventional ED defines a decision statistics with respect to PU signal presence or absence at the SU input based on determination of the log-LRT variance only. Definition of the jointly sufficient statistics of the GD log-LRT mean and variance allows us to make accurate decision about the PU signal presence or absence in comparison with the conventional MF, ED, correlation receiver and other modern signal detection algorithms. Theoretically, in the ideal case, the GD can be applied to detect any signal, i.e., the signal with known and unknown, deterministic or stochastic parameters under the very low SNR. The GD implementation in wireless communications and radar sensor systems is discussed in [24–31] and [32–38], respectively. Investigation concerning the GD employment in CR systems has been discussed in [39–41].

In this work with, the objective of spectrum sensing performance improving, i.e., the PU signal detection, at the low SNR under the spatial correlated antenna array elements, we proposed two spectrum sensing algorithms, namely, the weighted GD (WGD) and the generalized likelihood ratio test for the GD (GLRT-GD) when the noise variance is known and unknown, respectively. Both new algorithms are the blind detection approaches because these algorithms use only the received signal samples for detection, and can be classified or considered as eigenvalue based detectors owing to their test statistics depend on the sample covariance matrix eigenvalues. The simulation results confirm the effectiveness of implementation of the proposed algorithms in CR systems in comparison with WED, generalized likelihood ratio test for the ED (GLRT-ED), AGM, MME, EME, SLE, MBD, CBD, and max-min SNR detectors.

The conventional GD detection performance over different fading scenarios is not available in the related modern literature. Thus, the optimal GD detection threshold at the low SNR over the additive white Gaussian noise (AWGN), Nakagami-m, and Rayleigh fading channels is derived based on criterion of the minimum probability of error.

The remainder of this paper is organized as follows. Section 2 presents a general system model discussed in this paper. Brief description of the conventional GD structure and decision statistics are delivered in Section 3. The moment generation function (MGF) of partial decision statistics at the GD output is defined in Section 4. The proposed WGD and GLRT-GD decision statistics are discussed in Section 5. Definition of the GD optimal detection threshold for various types of fading channels is presented in Section 6. The simulation results confirming a theoretical analysis are presented and discussed in Section 7. Finally, the conclusion remarks are made in Section 8.

2. System model for antenna array sensing

One example of the CR system is presented in Fig. 1. We assume that the SU or secondary sensor node is equipped by antenna array with the number of elements equal to M. Each antenna array element receives N samples during the sensing time. The coarse spectrum sensing dilemma at the k-th time instant can be described by the conventional binary hypothesis test as follows:

$$\begin{cases} \mathcal{H}_0 = z_i[k] = w_i[k], & i = 1,\ldots,M; k = 0,\ldots,N-1, \\ \mathcal{H}_1 = z_i[k] = h_i[k]s[k] + w_i[k], & i = 1,\ldots,M; k = 0,\ldots,N-1, \end{cases} \tag{1}$$

where $\mathcal{H}_1$ is the hypothesis a "yes" PU signal; $\mathcal{H}_0$ is the alternative hypothesis; $z_i[k]$ is the discrete-time received signal at the SU or secondary sensor node input; $w_i[k]$ is the discrete-time circularly symmetric complex Gaussian noise with zero mean and variance σ_w^2, i.e., $w_i[k] \approx \mathcal{CN}(0, \sigma_w^2)$; $h_i[k]$ is the discrete-time channel coefficients obeying the circularly symmetric complex Gaussian distribution with zero mean and variance σ_h^2, i.e., $h_i[k] \approx \mathcal{CN}(0, \sigma_h^2)$; and $s[k]$ is the phase shift keying modulated signal transmitted by the PU with the same probability of transmission for each modulated symbol, and with the average received power E_s within the limits of the frequency band of interest. Throughout the paper, we

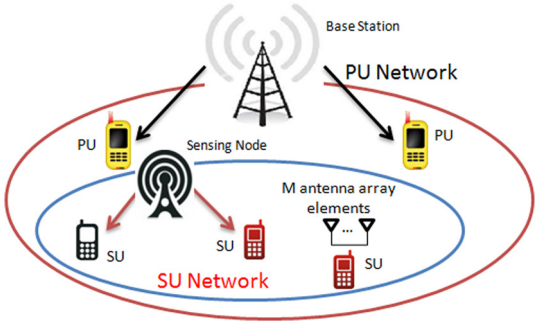

Fig. 1. Cognitive radio network and the secondary user SU with M elements of antenna array.

assume that the modulated signal $s[k]$, channel coefficients $h_i[k]$, and noise $w_i[k]$ are independent between each other. The channel coefficients $h_i[k]$ are spatially correlated between the antenna array elements but the channel parameters are not varied during the sensing time. The described channel model is discussed in detail in [42–44].

Owing to its simplicity, the exponential matrix model is widely used to describe the spatial correlation between the adjacent antenna array elements. The components of the antenna array element correlation matrix $\mathbf{R}$ with the size $M \times M$ can be presented in the following form [45]:

$$R_{ij} = \begin{cases} \rho^{i-j}, & i \le j \\ \rho^*_{ji}, & i > j \end{cases}, \quad i, j = 1, \ldots, M, \tag{2}$$

where ρ is the coefficient of spatial correlation between the adjacent antenna array elements, $0 \le \rho \le 1$ real values, and ρ^*_{ji} denotes the complex conjugate ($\rho_{ij} = \rho^*_{ji}$). Obviously, (2) may be not an accurate model for some real-world scenarios but this is a simple single-parameter model which allows us to study the effect of correlation on the MIMO capacity in an explicit way and to get some insight. The coefficient of correlation ρ can be determined using the approximated cross correlation function defined in [46]

$$\rho = \exp\left\{-23\Lambda^2 (d/\lambda)^2\right\}, \tag{3}$$

where Λ is the angular spread, an important propagation parameter defining a distribution of multipath power of radio waves coming in at the receiver input from a number of azimuthal directions with respect to the horizon; λ is the wavelength; and d is the distance between the adjacent antenna array elements (antenna array element spacing). The correlation matrix $\mathbf{R}$ of antenna array elements given by (2) is the symmetric Toeplitz matrix [42].

We define the $NM \times 1$ signal vector $\mathbf{Z}$ that collects the all observed signal samples during the sensing time using the following form:

$$\mathbf{Z} = \left[z_1(0), \ldots, z_M(0), \ldots, z_1(N-1), \ldots, z_M(N-1)\right]^T, \tag{4}$$

where T denotes a transpose. Since $s[k]$ has an equal probability of transmission for each modulated symbol as we mentioned before, then the complex vector $\mathbf{Z}$ has the $N \times M$ dimensional joint complex Gaussian distribution that can be expressed as [42]:

$$\mathbf{Z} = \begin{cases} \mathcal{CN}(0, \sigma_w^2 \mathbf{I}), & \Rightarrow \mathcal{H}_0 \\ \mathcal{CN}(0, E_s \sigma_h^2 \mathbf{\Sigma} + \sigma_w^2 \mathbf{I}), & \Rightarrow \mathcal{H}_1 \end{cases} \tag{5}$$

where E_s is the average energy of transmitted signal at the spectrum sensor input, and $\mathbf{I}$ is the $MN \times MN$ identity matrix. We consider a situation when the primary signaling scheme is unknown, i.e., the PU has a total freedom of choosing the signaling strategy, excepting a known power within the limits of the frequency band interest. Thus, the detector should be able to detect a presence of any possible PU signal $s[k]$ satisfying the power and bandwidth constraints for robust detection.

The received signal vector $\mathbf{Z}$ obeys the complex Gaussian distribution with the covariance matrices $\mathbf{Cov}_0$ and $\mathbf{Cov}_1$ at the hypotheses $\mathcal{H}_0$ and $\mathcal{H}_1$, respectively. If $z_i[k] = w_i[k]$, the received signals $z_i[k]$ are independent. Under the hypothesis $\mathcal{H}_1$, when $z_i[k] = h_i[k]s[k] + w_i[k]$ the received signals are spatially correlated. The covariance matrices $\mathbf{Cov}_0$ and $\mathbf{Cov}_1$ can be determined in the following form [3,42]:

$$\begin{cases} \mathbf{Cov}_0 = E[\mathbf{Z}\mathbf{Z}^H | \mathcal{H}_0] = \sigma_w^2 \mathbf{I}, \\ \mathbf{Cov}_1 = E[\mathbf{Z}\mathbf{Z}^H | \mathcal{H}_1] = E_s \sigma_h^2 \mathbf{\Sigma} \sigma_w^2 \mathbf{I}, \end{cases} \tag{6}$$

where $E[\cdot]$ is the mathematical expectation; H denotes the Hermitian conjugate (conjugate transpose); $\mathbf{I}$ is the $MN \times MN$ identity matrix; E_s is the PU average energy at the SU input; $\mathbf{\Sigma}$ is the $MN \times MN$ matrix defined based on the correlation matrix $\mathbf{R}$ given by (2) [45]:

$$\mathbf{\Sigma} = \begin{bmatrix} \mathbf{R} & \mathbf{0}_M & \cdots & \mathbf{0}_M \\ \mathbf{0}_M & \ddots & \ddots & \vdots \\ \vdots & \ddots & \ddots & \mathbf{0}_M \\ \mathbf{0}_M & \cdots & \mathbf{0}_M & \mathbf{R} \end{bmatrix}_{MN \times MN}, \tag{7}$$

here $\mathbf{0}_M$ are the $M \times M$ zero matrixes.

3. Conventional GD and related decision statistics

As we mentioned before, the GD is constructed in accordance with the GASP in noise [21–23]. The GD is considered as a linear combination of the correlation detector, which is optimal in the Neyman-Pearson criterion sense under detection of signals with a priori known parameters, and the ED, which is optimal under detection of signals with a priori unknown parameters or stochastic parameters. This GD feature allows us to obtain the better detection performance in comparison with other classical and modern receivers or detectors employed in practice.

The specific feature of GASP is introduction of the additional noise source that does not carry any information about the signal with the purpose to improve a qualitative signal detection performance. This additional noise can be considered as the reference noise without any information about the signal to be detected [21]. The jointly sufficient statistics of the log-LRT mean and variance is obtained in the case of GASP implementation, while the classical and modern signal processing theories can deliver only a sufficient statistics of the log-LRT mean or variance, i.e., not the jointly sufficient statistics of the log-LRT mean and variance. Thus, the GASP allows us to obtain more information about the received information signal, the PU signal. Owing to this fact, an implementation of receivers constructed based on GASP basis allows us to improve the spectrum sensing performance of CR wireless networks in comparison with employment of other conventional receivers at the SU.

The conventional GD flowchart is presented in Fig. 2. As we can see, the GD consists of three channels:

- The GD correlation channel (detector) – the preliminary filter (PF), multipliers 1 and 2, model signal generator MSG.
- The GD autocorrelation channel (GD ED) – the PF, additional filter (AF), multipliers 3 and 4, summator 1.
- The GD compensation channel – the summators 2, 3 and accumulator 1.

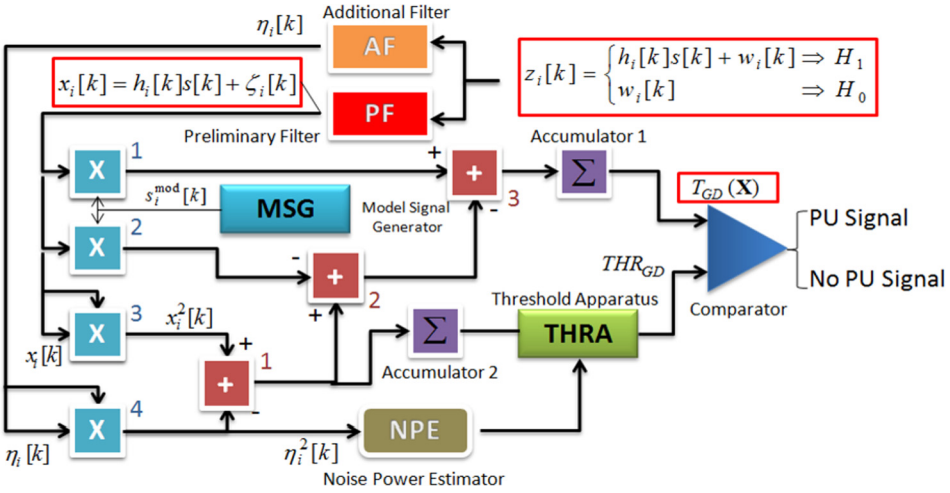

Fig. 2. GD structure: AF – additional filter; PF – preliminary filter; MSG – model signal generator; NPE – noise power estimation; THRA – threshold apparatus; PU Signal – primary user signal presence; No PU Signal – primary user signal absence.

The GD PF and AF are the bandpass filters (the linear discrete time systems) with the impulse responses $h_{PF}[m]$ and $h_{AF}[m]$, respectively. For simplicity of analysis, we assume that these filters have the same amplitude-frequency characteristics or impulse responses by shape. Moreover, the GD AF central frequency is detuned with respect to the GD PF one on such a value that the information signal, the PU signal, cannot pass through the GD AF. Thus, the PU signal and noise can be appeared at the GD PF output only and the only noise is appeared at the GD AF output. If a value of detuning between the GD AF and PF central frequencies is not less $4\Delta f_s$, where Δf_s is the PU signal bandwidth, the processes at the GD AF and PF outputs can be considered as the uncorrelated and independent processes and, in practice, under this condition, the coefficient of correlation between the GD PF and AF output processes is not more than 0.05 that was confirmed experimentally in [47] and [48].

In general, under practical implementation of any detector in spectrum sensing, the bandwidth of the spectrum to be sensed is defined. Thus, the GD AF bandwidth and central frequency can be assigned, too. In the present paper, we consider the spectrum sensing problem of a single radio channel where the GD AF bandwidth is always idle but it cannot be used by the SU because it is out of the useful spectrum of the considered primary network. There is a need to note that, in general case, the GD AF portion of the spectrum may be occupied by the PU signals from other networks, it is not unoccupied absolutely. In this case, such PU signals from other networks could be considered as interferences or interfering signals. The case when there are interfering signals with the limits of the GD AF bandwidth, the action of these interferences on the GD detection performance, and the case of non-ideal functioning condition for GD when the noise at the GD AF and PF are not identical by statistical parameters are discussed in [35].

In [21] under delivering the conventional GD decision statistics based on the likelihood ratio the processes at the GD AF and GD PF outputs were interpreted as the input stochastic samples generated by two independent sources. Thus, the GD AF can be considered as a reference noise generator with a priori knowledge a "no" signal, the reference sample noise. The GD PF can be considered as a generator with "a yes" signal (signal plus noise) or "a no" signal (noise only) sample. Detailed discussion of the GD AF and GD PF can be found in [21] and [22, Chapter 5]. The noise at the GD PF and GD AF outputs can be presented in the following form:

$$\begin{cases} w_{PF}[k] = \sum\limits_{i=1}^{M} \zeta_i[k] = \sum\limits_{m=-\infty}^{\infty} h_{PF}[m] w_i[k-m], \\ w_{AF}[k] = \sum\limits_{i=1}^{M} \eta_i[k] = \sum\limits_{m=-\infty}^{\infty} h_{AF}[m] w_i[k-m]. \end{cases} \tag{8}$$

As follows from Fig. 2, under the hypothesis $\mathcal{H}_1$, the GD ED generates PU signal energy $s_i^2[k]$ and the random component $s_i[k]\zeta_i[k]$ caused by interaction between the PU signal $s_i[k]$ and the noise $\zeta_i[k]$ at the GD PF output. The main purpose of the GD compensation channel is to cancel completely in the statistical sense the GD correlation channel noise component $s_i^{mod}[k]\zeta_i[k]$ and the GD ED random component $s_i[k]\zeta_i[k]$ between each other based on the same nature of the noise $\zeta_i[k]$.

The relation between the signal to be detected $s_i[k]$ and the model signal $s_i^{mod}[k]$ can be defined as:

$$s_i^{mod}[k] = \mu s_i[k], \tag{9}$$

where μ is the coefficient of proportionality. Satisfying the GD main functioning condition $s_i^{mod}[k] = s_i[k]$, i.e., $\mu = 1$ we are able to detect the PU signal with the high probability of detection at the low SNR and define the PU signal parameters with high accuracy. Practical realization of this condition requires increasing in the complexity of receiver structure and, consequently, leads us to increasing in the computational cost.

Under the hypothesis $\mathcal{H}_0$, i.e., a "no" PU signal, satisfying the GD main functioning condition given by (9), we obtain only the background noise $\eta_i^2[k] - \zeta_i^2[k]$ at the GD output. Additionally, the practical implementation of the GD decision statistics requires an estimation of the noise variance σ_w^2 using the reference noise $\eta_i[k]$ at the GD AF output. The threshold apparatus (THRA) device in Fig. 2 allows us to define the GD threshold. In the present paper, the GD circuitry is demonstrated with the purpose to explain the main functioning principles. Because of this, the GD flowchart presented in Fig. 2 must be considered under this viewpoint only.

The complete matching between the model signal $s_i^{mod}[k]$ and the incoming PU signal $s_i[k]$, for example, by amplitude is a very hard problem in practice because the incoming PU signal $s_i[k]$ depends on both the fading and the transmitted signal where it is impractical to estimate the fading gain at the low SNR. This matching is possible in the ideal case only. The GD detection performance will be deteriorated under mismatching between the model signal $s_i^{mod}[k]$ and the incoming PU signal $s_i[k]$ and the impact of this problem is discussed in [46], where the complete analy-

sis about the violation of the main GD functioning requirements is presented.

Under the hypothesis $\mathcal{H}_1$, the signal at the PF output, see Fig. 2, can be defined as $x_i[k] = s_i[k] + \zeta_i[k]$, where $s_i[k] = h_i[k]s[k]$. Under the hypothesis $\mathcal{H}_0$ and for all i and k, the process $x_i[k] = \zeta_i[k]$ at the PF output is subjected to the complex Gaussian distribution and can be considered as the independent and identically distributed (i.i.d.) process. In the ideal case, we can think that the signal at the GD AF output is the reference noise $\eta_i[k]$ with the same statistical parameters as the noise $\zeta_i[k]$. In practice, there is a difference between the statistical parameters of the noise $\eta_i[k]$ and $\zeta_i[k]$. How this difference impacts on the GD detection performance is discussed in detail in [22, Chapter 7, pp. 631–695].

The decision statistics at the GD output presented in [21] and [22] is extended to the case of antenna array employment when an adoption of multiple antennas and antenna arrays is effective to mitigate the negative attenuation and fading effects [32,33]. The decision statistics at the GD output can be presented in the following form:

$$T_{GD}(\mathbf{X}) = \sum_{k=0}^{N-1}\sum_{i=1}^{M} 2x_i[k]s_i^{\mathrm{mod}}[k] - \sum_{k=0}^{N-1} x_i^2[k] + \sum_{k=0}^{N-1}\sum_{i=1}^{M} \eta_i^2[k] \gtrless_{\mathcal{H}_0}^{\mathcal{H}_1} THR_{GD}, \tag{10}$$

where THR_{GD} is the GD detection threshold. We can rewrite (10) in the matrix form as follows:

$$T_{GD}(\mathbf{X}) = 2\mathbf{S}^{\mathrm{mod}}\mathbf{X} - \mathbf{X}^2 + \boldsymbol{\eta}^2 \gtrless_{\mathcal{H}_0}^{\mathcal{H}_1} THR_{GD}, \tag{11}$$

where

$$\mathbf{X} = \{\mathbf{x}[0], \ldots, \mathbf{x}[N-1]\} \tag{12}$$

is the $M \times 1$ matrix of the stochastic process at the GD PF output with the elements defined as

$$\mathbf{x}[k] = \{x_1[k], \ldots, x_M[k]\}^T; \tag{13}$$

$$\mathbf{S}^{\mathrm{mod}} = \{\mathbf{s}^{\mathrm{mod}}[0], \ldots, \mathbf{s}^{\mathrm{mod}}[N-1]\} \tag{14}$$

is the $M \times 1$ matrix of the process at the MSG output with the elements defined as

$$\mathbf{s}^{\mathrm{mod}}[k] = \{s_1^{\mathrm{mod}}[k], \ldots, s_M^{\mathrm{mod}}[k]\}^T; \tag{15}$$

$$\boldsymbol{\eta} = \{\boldsymbol{\eta}[0], \ldots, \boldsymbol{\eta}[N-1]\} \tag{16}$$

is the $M \times 1$ matrix of the stochastic process at the GD AF output with the elements defined as

$$\boldsymbol{\eta}[k] = \{\eta_1[k], \ldots, \eta_M[k]\}^T. \tag{17}$$

According to the GASP and GD flowchart shown in Fig. 2, the GD decision statistics takes the following form under the hypotheses $\mathcal{H}_1$ and $\mathcal{H}_0$, respectively:

$$T_{GD}(\mathbf{X}) = \begin{cases} \sum_{k=0}^{N-1}\sum_{i=1}^{M} s_i^2[k] + \sum_{k=0}^{N-1}\sum_{i=1}^{M} \eta_i^2[k] - \sum_{k=0}^{N-1}\sum_{i=1}^{M} \zeta_i^2[k] \Rightarrow \mathcal{H}_1, \\ \sum_{k=0}^{N-1}\sum_{i=1}^{M} \eta_i^2[k] - \sum_{k=0}^{N-1}\sum_{i=1}^{M} \zeta_i^2[k] \Rightarrow \mathcal{H}_0. \end{cases} \tag{18}$$

The term $\sum_{k=0}^{N-1}\sum_{i=1}^{M} s_i^2[k]$ is the average energy of the received PU signal and the term $\sum_{k=0}^{N-1}\sum_{i=1}^{M} \eta_i^2[k] - \sum_{k=0}^{N-1}\sum_{i=1}^{M} \zeta_i^2[k]$ presents the background noise at the GD output that is a difference between the noise power at the GD PF and GD AF outputs.

The mean $m_{\mathcal{H}_0}^{GD}$ and variance $Var_{\mathcal{H}_0}^{GD}$ of the decision statistics $T_{GD}(\mathbf{X})$ at the GD output under consideration of the hypothesis $\mathcal{H}_0$ are given in the following form [25, Chapter 3]:

$$\begin{cases} m_{\mathcal{H}_0}^{GD} = E[T_{GD}(\mathbf{X})|\mathcal{H}_0] = 0, \\ Var_{\mathcal{H}_0}^{GD} = Var[T_{GD}(\mathbf{X})|\mathcal{H}_0] = 4NM\sigma_w^4. \end{cases} \tag{19}$$

The above-mentioned discussion is correct for the case when the noise variance at the GD AF and GD PF outputs is the same, i.e., $\sigma_\zeta^2 = \sigma_\eta^2 = \sigma_w^2$. For the case that is very close to practice if the GD AF and GD PF are the band pass filters with deviation in parameters, i.e., $\sigma_\zeta^2 \neq \sigma_\eta^2$, we can assume $\sigma_\zeta^2 = \sigma_w^2$ and $\sigma_\eta^2 = \beta\sigma_\zeta^2 = \beta\sigma_w^2$. For this case, (19) takes the following form:

$$\begin{cases} m_{\mathcal{H}_0}^{GD} = E[T_{GD}(\mathbf{X})|\mathcal{H}_0] = 0, \\ Var_{\mathcal{H}_0}^{GD} = Var[T_{GD}(\mathbf{X})|\mathcal{H}_0] = 2NM\sigma_w^4(1+\beta^2). \end{cases} \tag{20}$$

In the present paper, we discuss the GD implementation as a spectrum sensor in CR systems, i.e., coarse sensing. Detailed discussion about the main GD functioning principles if there is no a priori information about the PU signal and there is an uncertainty about the PU signal parameters, i.e., the PU signal parameters are stochastic, can be found in [21] and [22, Chapter 6, pp. 611–621 and Chapter 7, pp. 631–695].

4. MGF of the decision statistics at the GD output

The moment generating function (MGF) for the GD partial decision statistics $T_{GD}(\mathbf{X}_k)$ under the hypothesis $\mathcal{H}_1$ given by

$$T_{GD}(\mathbf{X}_k) = \sum_{i=1}^{M} s_i^2[k] + \sum_{i=1}^{M} \eta_i^2[k] - \sum_{i=1}^{M} \zeta_i^2[k] \tag{21}$$

is required. This MGF can be presented in the following form (see Appendix 2):

$$\begin{aligned} &\mathcal{M}_{T_{GD}(\mathbf{X}_k)}(l) \\ &= \prod_{i=1}^{M}\left[1 - E_s\sigma_h^2\alpha_i l\right]^{-1} \prod_{i=1}^{M} \mathcal{M}_{z_{1_i}}(l) \prod_{i=1}^{M} \mathcal{M}_{z_{2_i}}(-l) \\ &= \prod_{i=1}^{M}\left[1 - E_s\sigma_h^2\alpha_i l\right]^{-1} \prod_{i=1}^{M}\left(1 - 2\sigma_w^2 l\right)^{-0.5} \prod_{i=1}^{M}\left(1 + 2\sigma_w^2 l\right)^{-0.5} \\ &= \prod_{i=1}^{M}\left[1 - E_s\sigma_h^2\alpha_i l\right]^{-1} \left(1 - 2\sigma_w^2 l\right)^{-0.5M} \left(1 + 2\sigma_w^2 l\right)^{-0.5M} \\ &= \left(1 - 4\sigma_w^4 l^2\right)^{-0.5M} \prod_{i=1}^{M}\left[1 - E_s\sigma_h^2\alpha_i l\right]^{-1}, \end{aligned} \tag{22}$$

where α_i is the eigenvalue of the correlation matrix $\mathbf{R}$ given by (2) for the i-th spatial channel. Based on (22) and taking into consideration results discussed in [33], the mean and variance of the GD partial decision statistics $T_{GD}(\mathbf{X}_k)$ under the hypothesis $\mathcal{H}_1$ take the following form, respectively:

$$\begin{cases} m_{\mathcal{H}_1}^{GD} = E[T_{GD}(\mathbf{X})|\mathcal{H}_1] = NME_s\sigma_h^2, \\ Var_{\mathcal{H}_1}^{GD} = Var[T_{GD}(\mathbf{X})|\mathcal{H}_1] = N\left[\sum_{i=1}^{M} E_s^2\sigma_h^4\alpha_i^2 + 4M\sigma_w^4\right]. \end{cases} \tag{23}$$

For the case $\sigma_\zeta^2 \neq \sigma_\eta^2$, (23) takes the following form:

$$\begin{cases} m_{\mathcal{H}_1}^{GD} = E[T_{GD}(\mathbf{X})|\mathcal{H}_1] = NME_s\sigma_h^2, \\ Var_{\mathcal{H}_1}^{GD} = Var[T_{GD}(\mathbf{X})|\mathcal{H}_1] = N\left[\sum_{i=1}^{M} E_s^2\sigma_h^4\alpha_i^2 + 2M\sigma_w^4(1+\beta^2)\right]. \end{cases} \tag{24}$$

We consider the case when a relation between the model signal and incoming PU signal can be presented by (9) if the coefficient of proportionality equal to μ. Under the condition (9), the MGF of the GD partial decision statistics

$$T_{GD}(\mathbf{X}_k) = \sum_{i=1}^{M} s_i^2[k](2\mu-1) + \sum_{i=1}^{M} 2s_i[k]\xi_i[k](\mu-1) + \sum_{i=1}^{M}\eta_i^2[k] - \sum_{i=1}^{M}\xi_i^2[k] \tag{25}$$

takes the following form:

$$\begin{aligned} &\mathcal{M}_{T_{GD}(\mathbf{x}_k)}(l) \\ &= \prod_{i=1}^{M}\left[1 - E_s\sigma_h^2 l(2\mu-1)\right]^{-1} \prod_{i=1}^{M}\left[1 - 2l(\mu-1)\sqrt{E_s\sigma_h^2\sigma_w^2}\right]^{-1} \\ &\quad \times \left(1 - 2\sigma_w^2 l\right)^{-0.5M}\left(1 + 2\sigma_w^2 l\right)^{-0.5M}. \end{aligned} \tag{26}$$

Based on (26), the mean $m_{\mathcal{H}_1}^{GD}$ and variance $Var_{\mathcal{H}_1}^{GD}$ of the GD partial decision statistics $T_{GD}(\mathbf{X}_k)$ under the hypothesis $\mathcal{H}_1$ are defined using the following form:

$$\begin{cases} m_{\mathcal{H}_1}^{GD} = E[T_{GD}(\mathbf{X})|\mathcal{H}_1] = NM(2\mu-1)E_s\sigma_h^2; \\ Var_{\mathcal{H}_1}^{GD} = Var[T_{GD}(\mathbf{X})|\mathcal{H}_1] \\ \quad = N\left\{\sum_{i=1}^{M}\left[(2\mu-1)^2E_s^2\sigma_h^2\alpha_i^2 + 4(\mu-1)^2E_s\sigma_h^2\alpha_i\sigma_w^2\right] + 4\sigma_w^4\right\}; \\ \quad \sigma_\zeta^2 = \sigma_\eta^2 = \sigma_w^2; \end{cases} \tag{27}$$

$$\begin{cases} m_{\mathcal{H}_1}^{GD} = E[T_{GD}(\mathbf{X})|\mathcal{H}_1] = NM(2\mu-1)E_s\sigma_h^2; \\ Var_{\mathcal{H}_1}^{GD} = Var[T_{GD}(\mathbf{X})|\mathcal{H}_1] \\ \quad = N\left\{\sum_{i=1}^{M}\left[(2\mu-1)^2E_s^2\sigma_h^2\alpha_i^2 + 2(\mu-1)^2E_s\sigma_h^2\alpha_i\sigma_w^2(1+\beta)\right]\right. \\ \qquad \left. + 2\sigma_w^4(1+\beta^2)\right\}; \sigma_\zeta^2 \neq \sigma_\eta^2. \end{cases} \tag{28}$$

5. WGD and GLRT-GD: correlated antenna array elements

Finally, the weighted GD (WGD) decision statistics can be determined using the following form (see Appendix 1):

$$\begin{aligned} T_{WGD}(\mathbf{X}) &= \ln L_{GD}(\mathbf{X}) \\ &= \sum_{k=0}^{N-1}\sum_{i=1}^{M}\frac{E_s\sigma_h^2\alpha_i}{2\sigma_w^2(E_s\sigma_h^2\alpha_i + \sigma_w^2)}y_i^2[k] \\ &\quad - \frac{N}{2\sigma_w^2}\left[\sum_{i=1}^{M}\lambda_{R_x i} - \sum_{i=1}^{M}\lambda_{R_\eta i}\right] \\ &= \sum_{k=0}^{N-1}\sum_{i=1}^{M}\frac{\gamma\alpha_i}{2\sigma_w^2(\gamma\alpha_i+1)}y_i^2[k] \\ &\quad - \frac{N}{2\sigma_w^2}\left[\sum_{i=1}^{M}\lambda_{R_x i} - \sum_{i=1}^{M}\lambda_{R_\eta i}\right] \gtrless_{\mathcal{H}_0}^{\mathcal{H}_1} THR_{WGD}, \end{aligned} \tag{29}$$

where THR_{WGD} is the decision statistics threshold, and

$$\gamma = \frac{E_s\sigma_h^2}{\sigma_w^2} \tag{30}$$

is the SNR at the GD input. We see from (30) that the weighting coefficients $\gamma\alpha_i/(\gamma\alpha_i+1)$ are actually similar to the Wiener filter weights in a transformed space [3]. The effect of the linear transformation $\mathbf{X}[k]$ to $\mathbf{Y}[k]$ is to decorrelate the matrix $\mathbf{X}$ of the random process at the GD PF output.

For the better understanding, let us define the covariance matrix $\mathbf{R}_Y[k]$ of the transmitted data $\mathbf{Y}[k]$ under each hypothesis. Under the hypothesis $\mathcal{H}_1$ we have:

$$\begin{aligned} \mathbf{R}_Y^{\mathcal{H}_1}[k] &= E\left\{\mathbf{V}^H\mathbf{X}[k]\mathbf{X}^H[k]\mathbf{V}\right\} = \mathbf{V}^H\left(\mathbf{R} + \sigma_w^2\mathbf{I}\right)\mathbf{V} \\ &= \mathbf{V}^H\mathbf{R}\mathbf{V} + \sigma_w^2\mathbf{I} = \mathbf{\Lambda} + \sigma_w^2\mathbf{I}. \end{aligned} \tag{31}$$

We can see that $\mathbf{R}_Y^{\mathcal{H}_1}[k]$ is a diagonal matrix. Similarly, under the hypothesis $\mathcal{H}_0$ we can find that

$$\mathbf{R}_Y^{\mathcal{H}_0}[k] = \sigma_w^2\mathbf{I}. \tag{32}$$

Hence, the process $\mathbf{Y}[k]$ consists of uncorrelated random variables and owing to the fact that the variances of these random variables are not equal between each other the WGD weights the squares of $y_i[k]$ differently. Thus, the components of $\mathbf{X}[k]$ are likely to be much larger when the PU signal is present in comparison with the case when the PU signal is absent. As a result, the WGD employment helps us to reduce the spatial correlation between the antenna array elements and improve the signal detection performance.

Based on (109) and (114) (see Appendix 1) the GLRT-GD decision statistics takes the following form:

$$\begin{aligned} &T_{GD}^{GLRT}\left(\mathbf{Y} = \mathbf{V}^H\mathbf{X}\right) \\ &= \ln L_{GD}^{GLRT}(\mathbf{Y}) = \frac{NM}{2}\ln\hat{\sigma}_0^2 - \frac{N}{2}\sum_{i=1}^{M}\ln\hat{\sigma}_1^2(\gamma\lambda_i+1) \\ &\quad - \sum_{k=0}^{N-1}\sum_{i=1}^{M}\frac{y_i^2[k]}{2\hat{\sigma}_1^2(\gamma\lambda_i+1)} + \sum_{k=0}^{N-1}\frac{\boldsymbol{\eta}^H[k]\boldsymbol{\eta}[k]}{2\hat{\sigma}_0^2\mathbf{I}}. \end{aligned} \tag{33}$$

The test statistics of the proposed spectrum sensing approaches, namely, the weighted GD (WGD) and GLRT-GD can increase the degree of knowledge needed for the PU signal detection by introducing two sample covariance matrices of the data samples at the outputs of GD PF and GD AF. Moreover, the eigen-decomposition is applied to represent these sample covariance matrices in terms of eigenvalues and eigenvectors (the matrix factorization into a canonical form) that adds even more effectiveness to the noise power MLEs performance designed for GLRT-GD approach.

The noise power is estimated applying consistent MLE in real time using the reference noise samples $\boldsymbol{\eta} = \{\boldsymbol{\eta}[0], \ldots, \boldsymbol{\eta}[N-1]\}$ at the GD AF output in the case of GLRT-GD. The direct impacts can be observed on the spectrum sensing performance of this approach as a consequence of the better noise power estimation accuracy, i.e., the smaller estimation error, which leads to the better detection threshold definition alleviating the effect of noise power uncertainty and the related SNR wall problem when increasing the number of samples or sensing time will not improve sensing performance. Thus, the GLRT-GD can calibrate the noise power uncertainty under estimation process by the compensation channel using the reference noise forming at the GD AF output and detect the PU signal at low SNR values (see Section 7, Figs. 3–8, 12).

6. Optimal GD detection threshold: fading channels

The performance of any detector is evaluated by the probability of detection P_D, bit error rate (BER), probability of false alarm P_{FA}, probability of error P_{error}, and probability of miss P_{miss}. The detection threshold is the main parameter used to determine these probabilities. In general, it is desirable to achieve the high probability of detection P_D keeping the probability of false alarm P_{FA} as small as possible. A choice of the detection threshold can be carried out based on various objectives such as the total error rate minimization [49]. We derive the optimal detection threshold in the case of the conventional GD for different fading channels minimizing the probability of error P_{error}.

6.1. AWGN fading channel

The GD decision statistics $T_{GD}(\mathbf{X})$ under consideration of the hypothesis $\mathcal{H}_0$ is the sum of i.i.d. $N \times M$ random variables obeyed to the McDonald's distribution [22, Chapter 3, pp. 250–263]. We can approximate the probability density function (pdf) of the GD decision statistics $T_{GD}(\mathbf{X})$ by the normal Gaussian distribution law based on the central limit theorem as $N \to \infty$. The central limit theorem can give a reasonable approximation for the original pdf if the number of samples is sufficiently large, in practice, $N \times M \gg 10$ [42]. As a result, the GD decision statistics $T_{GD}(\mathbf{X})$ is the sum of i.i.d. random variables and the central limit theorem can be applied to define the pdf of the decision statistics at the GD output if the number of observed samples is large. In line with, we can define the probability of false alarm P_{FA}^{GD} and the probability of detection P_D^{GD} as follows [23]:

$$P_{FA}^{GD} = P\left[T_{GD}(\mathbf{X}) \geq THR_{GD} | \mathcal{H}_0\right] = Q\left(\frac{THR_{GD} - m_{\mathcal{H}_0}^{GD}}{\sqrt{Var_{\mathcal{H}_0}^{GD}}}\right), \tag{34}$$

$$P_D^{GD} = P\left[T_{GD}(\mathbf{X}) \geq THR_{GD} | \mathcal{H}_1\right] = Q\left(\frac{THR_{GD} - m_{\mathcal{H}_1}^{GD}}{\sqrt{Var_{\mathcal{H}_1}^{GD}}}\right), \tag{35}$$

where

$$Q(x) = \frac{1}{\sqrt{2\pi}} \int_x^{\infty} \exp\left(-0.5t^2\right) dt \tag{36}$$

is the Marcum Q-function; $m_{\mathcal{H}_0}^{GD}$ and $Var_{\mathcal{H}_0}^{GD}$ are the mean and variance of the decision statistics $T_{GD}(\mathbf{X})$ under the hypothesis $\mathcal{H}_0$, respectively; $m_{\mathcal{H}_1}^{GD}$ and $Var_{\mathcal{H}_1}^{GD}$ are the mean and variance of the decision statistics $T_{GD}(\mathbf{X})$ under the hypothesis $\mathcal{H}_1$, respectively. In the case of the hypothesis $\mathcal{H}_0$, the mean $m_{\mathcal{H}_0}^{GD}$ and variance $Var_{\mathcal{H}_0}^{GD}$ of the decision statistics $T_{GD}(\mathbf{X})$ are given by (19), $s_i^{\text{mod}}[k] = s_i[k] = 0$, $\sigma_\zeta^2 = \sigma_\eta^2$ and (20), $s_i^{\text{mod}}[k] = s_i[k] = 0$, $\sigma_\zeta^2 \neq \sigma_\eta^2$, i.e., $\sigma_\zeta^2 = \sigma_w^2$ and $\sigma_\eta^2 = \beta\sigma_w^2$. Under the hypothesis $\mathcal{H}_1$, the mean $m_{\mathcal{H}_1}^{GD}$ and variance $Var_{\mathcal{H}_1}^{GD}$ of the decision statistics $T_{GD}(\mathbf{X})$ are given by (23) at the condition $s_i^{\text{mod}}[k] = \mu s_i[k]$, $\mu = 1$, $\sigma_\zeta^2 = \sigma_\eta^2$, (24) at the condition $s_i^{\text{mod}}[k] = \mu s_i[k]$, $\mu = 1$, $\sigma_\zeta^2 \neq \sigma_\eta^2$, i.e., $\sigma_\zeta^2 = \sigma_w^2$ and $\sigma_\eta^2 = \beta\sigma_w^2$; (27) at the condition $s_i^{\text{mod}}[k] = \mu s_i[k]$, $\mu \neq 1$, $\sigma_\zeta^2 = \sigma_\eta^2$, and (28), i.e., $s_i^{\text{mod}}[k] = \mu s_i[k]$, $\mu \neq 1$, $\sigma_\zeta^2 \neq \sigma_\eta^2$, i.e., $\sigma_\zeta^2 = \sigma_w^2$ and $\sigma_\eta^2 = \beta\sigma_w^2$.

Based on the above-mentioned discussion, the GD decision threshold THR_{GD} when there is the constraint δ for the probability of detection P_D^{GD} can be determined in the following form:

The case 1: $s_i^{\text{mod}}[k] = \mu s_i[k]$, $\mu = 1$, $\sigma_\zeta^2 = \sigma_\eta^2$. Using (23) and taking into consideration a definition for SNR given by (30) we have

$$\begin{aligned} THR_{GD} &= m_{\mathcal{H}_1}^{GD} + \sqrt{Var_{\mathcal{H}_1}^{GD}}\, Q^{-1}(\delta) \\ &= NME_s\sigma_h^2 + Q^{-1}(\delta)\sqrt{N\left[\sum_{i=1}^{M} E_s^2\sigma_h^4\alpha_i^2 + 4M\sigma_w^4\right]} \\ &= NM\gamma\sigma_w^2 + Q^{-1}(\delta)\sqrt{N\left[\sum_{i=1}^{M} \gamma^2\sigma_w^4\alpha_i^2 + 4M\sigma_w^4\right]} \\ &= \sigma_w^2\left\{NM\gamma + Q^{-1}(\delta)\sqrt{N\left[\sum_{i=1}^{M} \gamma^2\alpha_i^2 + 4M\right]}\right\}. \end{aligned} \tag{37}$$

The case 2: $s_i^{\text{mod}}[k] = \mu s_i[k]$, $\mu = 1$, $\sigma_\zeta^2 \neq \sigma_\eta^2$, i.e., $\sigma_\zeta^2 = \sigma_w^2$ and $\sigma_\eta^2 = \beta\sigma_w^2$. Using (24) and taking into consideration a definition for SNR given by (30) we obtain

$$\begin{aligned} THR_{GD} &= m_{\mathcal{H}_1}^{GD} + \sqrt{Var_{\mathcal{H}_1}^{GD}}\, Q^{-1}(\delta) \\ &= NME_s\sigma_h^2 + Q^{-1}(\delta)\sqrt{N\left[\sum_{i=1}^{M} E_s^2\sigma_h^4\alpha_i^2 + 2M\sigma_w^4\left(1+\beta^2\right)\right]} \\ &= NM\gamma\sigma_w^2 + Q^{-1}(\delta)\sqrt{N\left[\sum_{i=1}^{M} \gamma^2\sigma_w^4\alpha_i^2 + 2M\sigma_w^4\left(1+\beta^2\right)\right]} \\ &= \sigma_w^2\left\{NM\gamma + Q^{-1}(\delta)\sqrt{N\left[\sum_{i=1}^{M} \gamma^2\alpha_i^2 + 2M\left(1+\beta^2\right)\right]}\right\}. \end{aligned} \tag{38}$$

The case 3: $s_i^{\text{mod}}[k] = \mu s_i[k]$, $\mu \neq 1$, $\sigma_\zeta^2 = \sigma_\eta^2$. Using (27) and taking into consideration a definition for SNR given by (30) we obtain

$$\begin{aligned} THR_{GD} &= m_{\mathcal{H}_1}^{GD} + \sqrt{Var_{\mathcal{H}_1}^{GD}}\, Q^{-1}(\delta) \\ &= NM(2\mu-1)E_s\sigma_h^2 + Q^{-1}(\delta) \\ &\times \sqrt{N\left[\sum_{i=1}^{M}\left[(2\mu-1)^2E_s^2\sigma_h^4\alpha_i^2 + 4(\mu-1)^2E_s\sigma_h^2\sigma_w^2\alpha_i^2\right] + 4M\sigma_w^4\right]} \\ &= \sqrt{NM}\sigma_w^2\left\{\sqrt{NM}(2\mu-1)\gamma\right. \\ &\left. + Q^{-1}(\delta)\sqrt{\frac{1}{M}\sum_{i=1}^{M}\left[(2\mu-1)^2\gamma^2\alpha_i^2 + 4(\mu-1)^2\gamma\alpha_i\right] + 4}\right\}. \end{aligned} \tag{39}$$

The case 4: $s_i^{\text{mod}}[k] = \mu s_i[k]$, $\mu \neq 1$, $\sigma_\zeta^2 \neq \sigma_\eta^2$, i.e., $\sigma_\zeta^2 = \sigma_w^2$ and $\sigma_\eta^2 = \beta\sigma_w^2$. Using (28) and taking into consideration a definition for SNR given by (30) we obtain

$$\begin{aligned} &THR_{GD} = m_{\mathcal{H}_1}^{GD} + \sqrt{Var_{\mathcal{H}_1}^{GD}}\, Q^{-1}(\delta) \\ &= NM(2\mu-1)E_s\sigma_h^2 + Q^{-1}(\delta) \\ &\times \sqrt{N\left[\sum_{i=1}^{M}\left[(2\mu-1)^2E_s^2\sigma_h^4\alpha_i^2 + 2(\mu-1)^2E_s\sigma_h^2\alpha_i\sigma_w^2(1+\beta)\right] + 2M\sigma_w^4\left(1+\beta^2\right)\right]} \\ &= \sqrt{NM}\sigma_w^2\left\{\sqrt{NM}(2\mu-1)\gamma\right. \\ &\left. + Q^{-1}(\delta)\sqrt{\frac{1}{M}\sum_{i=1}^{M}\left[(2\mu-1)^2\gamma^2\alpha_i^2 + 2(\mu-1)^2\gamma\alpha_i(1+\beta)\right] + 2\left(1+\beta^2\right)}\right\}. \end{aligned} \tag{40}$$

The constraint δ is required to maintain the predetermined lower bound of the probability of detection P_D^{GD} with the purpose to avoid a generation of interference under the PU signal transmission, in other words, $P_D^{GD} \geq \delta$. The detection threshold in (60)–(63) is a theoretical presentation used for definition of the probability of false alarm P_{FA}^{GD} at the probability of detection constraint $P_D^{GD} \geq \delta$.

Substituting (19), (20), (37)–(40) into (34) we obtain that the probability of false alarm P_{FA}^{GD} for the correlated antenna array elements can be presented in the following form:

The case 1: $s_i^{\text{mod}}[k] = \mu s_i[k]$, $\mu = 1$, $\sigma_\zeta^2 = \sigma_\eta^2$.

$$P_{FA}^{GD_{cor}} = Q\left\{\frac{1}{2}\left[\sqrt{NM}\gamma + Q^{-1}(\delta)\sqrt{\frac{1}{M}\left[\sum_{i=1}^{M}\gamma^2\alpha_i^2 + 4M\right]}\right]\right\}, \tag{41}$$

where γ is the SNR at the GD input given by (30). As follows from (64), the probability of false alarm P_{FA}^{GD} for the uncorrelated independent antenna array elements can be presented in the following form:

$$P_{FA}^{GD_{uncor}} = \lim_{\rho\to 0} P_{FA}^{GD_{cor}} = Q\left\{\frac{1}{2}\left[\sqrt{NM}\gamma + Q^{-1}(\delta)\sqrt{\gamma^2+4}\right]\right\}. \tag{42}$$

The case 2: $s_i^{\text{mod}}[k] = \mu s_i[k]$, $\mu = 1$, $\sigma_\zeta^2 \neq \sigma_\eta^2$, i.e., $\sigma_\zeta^2 = \sigma_w^2$ and $\sigma_\eta^2 = \beta\sigma_w^2$.

$$P_{FA}^{GD_{cor}} = Q\left\{\frac{1}{2}\left[\sqrt{NM}\gamma + Q^{-1}(\delta)\sqrt{\frac{1}{M}\left[\sum_{i=1}^{M}\gamma^2\alpha_i^2 + 2M\left(1+\beta^2\right)\right]}\right]\right\}. \tag{43}$$

As follows from (43), the probability of false alarm P_{FA}^{GD} for the uncorrelated independent antenna array elements can be presented in the following form:

$$P_{FA}^{GD_{uncor}} = \lim_{\rho\to 0} P_{FA}^{GD_{cor}} = Q\left\{\frac{1}{2}\left[\sqrt{NM}\gamma + Q^{-1}(\delta)\sqrt{\gamma^2+2M\left(1+\beta^2\right)}\right]\right\}. \tag{44}$$

The case 3: $s_i^{\text{mod}}[k] = \mu s_i[k]$, $\mu \neq 1$, $\sigma_\zeta^2 = \sigma_\eta^2$.

$$P_{FA}^{GD_{cor}} = Q\left\{\frac{1}{2}\left[\sqrt{NM}(2\mu-1)\gamma + Q^{-1}(\delta) \times \sqrt{\frac{1}{M}\left[\sum_{i=1}^{M}\left[(2\mu-1)^2\gamma^2\alpha_i^2 + 4(\mu-1)^2\gamma\alpha_i\right] + 4\right]}\right]\right\}. \tag{45}$$

As follows from (45), the probability of false alarm P_{FA}^{GD} for the uncorrelated independent antenna array elements can be presented in the following form:

$$P_{FA}^{GD_{uncor}} = \lim_{\rho\to 0} P_{FA}^{GD_{cor}} = Q\left\{\frac{1}{2}\left[\sqrt{NM}(2\mu-1)\gamma + Q^{-1}(\delta)\sqrt{(2\mu-1)^2\gamma^2\alpha_i^2 + 4(\mu-1)^2\gamma\alpha_i + 4}\right]\right\}. \tag{46}$$

The case 4: $s_i^{\text{mod}}[k] = \mu s_i[k]$, $\mu \neq 1$, $\sigma_\zeta^2 \neq \sigma_\eta^2$, i.e., $\sigma_\zeta^2 = \sigma_w^2$ and $\sigma_\eta^2 = \beta\sigma_w^2$.

$$P_{FA}^{GD_{cor}} = Q\left\{\frac{1}{2}\left[\sqrt{NM}(2\mu-1)\gamma + Q^{-1}(\delta) \times \sqrt{\frac{1}{M}\left[\sum_{i=1}^{M}\left[(2\mu-1)^2\gamma^2\alpha_i^2 + 2(\mu-1)^2\gamma\alpha_i(1+\beta)\right] + 2\left(1+\beta^2\right)\right]}\right]\right\}. \tag{47}$$

As follows from (47), the probability of false alarm P_{FA}^{GD} for the uncorrelated independent antenna array elements can be presented in the following form:

$$P_{FA}^{GD_{uncor}} = \lim_{\rho\to 0} P_{FA}^{GD_{cor}} = Q\left\{\frac{1}{2}\left[\sqrt{NM}(2\mu-1)\gamma + Q^{-1}(\delta) \times \sqrt{(2\mu-1)^2\gamma^2\alpha_i^2 + 2(\mu-1)^2\gamma\alpha_i(1+\beta) + 2\left(1+\beta^2\right)}\right]\right\}. \tag{48}$$

In the case of AWGN channel, the GD optimal threshold is defined based on the minimal probability of error P_{error}^{GD} given, in general case, as

$$P_{error_{AWGN}}^{GD} = p_0 P_{FA}^{GD} + p_1 P_{miss}^{GD}, \tag{49}$$

where

$$P_{miss}^{GD} = 1 - P_D^{GD} \tag{50}$$

is the probability of miss, p_0 and $p_1 = 1 - p_0$ are the a priori probabilities of the PU signal absence and presence at the GD input, respectively. For simplicity of analysis, we assume that these a priori probabilities are equal between each other, i.e., $p_0 = p_1 = 0.5$. Thus, we can write

$$THR_{GD_{AWGN}}^{op} = \arg\min_{THR_{GD}} P_{error}^{GD}(THR_{GD}). \tag{51}$$

Consider the case when the antenna array elements are uncorrelated. In this case, taking into consideration (19), (20), (27), (28), and (35) (51) can be presented in the following form:

The case 1: $s_i^{\text{mod}}[k] = \mu s_i[k]$, $\mu = 1$, $\sigma_\zeta^2 = \sigma_\eta^2$.

$$THR_{GD_{AWGN}}^{op} = \arg\min_{THR_{GD}} \frac{1}{2}\left\{1 - \frac{1}{2}\,\text{erfc}\left\{\frac{THR_{GD} - NM\gamma\sigma_w^2}{\sigma_w^2\sqrt{2NM(\gamma^2+4)}}\right\} + \frac{1}{2}\,\text{erfc}\left\{\frac{THR_{GD}}{2\sigma_w^2\sqrt{2NM}}\right\}\right\}. \tag{52}$$

The case 2: $s_i^{\text{mod}}[k] = \mu s_i[k]$, $\mu = 1$, $\sigma_\zeta^2 \neq \sigma_\eta^2$, i.e., $\sigma_\zeta^2 = \sigma_w^2$ and $\sigma_\eta^2 = \beta\sigma_w^2$.

$$THR_{GD_{AWGN}}^{op} = \arg\min_{THR_{GD}} \frac{1}{2}\left\{1 - \frac{1}{2}\,\text{erfc}\left\{\frac{THR_{GD} - NM\gamma\sigma_w^2}{\sigma_w^2\sqrt{2NM[\gamma^2+2(1+\beta^2)]}}\right\} + \frac{1}{2}\,\text{erfc}\left\{\frac{THR_{GD}}{2\sigma_w^2\sqrt{2NM(1+\beta^2)}}\right\}\right\}. \tag{53}$$

The case 3: $s_i^{\text{mod}}[k] = \mu s_i[k]$, $\mu \neq 1$, $\sigma_\zeta^2 = \sigma_\eta^2$.

$$THR_{GD_{AWGN}}^{op} = \arg\min_{THR_{GD}} \frac{1}{2}\left\{1 - \frac{1}{2}\operatorname{erfc}\left\{\frac{THR_{GD} - NM\gamma\sigma_w^2(2\mu-1)}{\sigma_w^2\sqrt{2NM[(2\mu-1)^2\gamma^2 + 4(\mu-1)^2\gamma + 4]}}\right\} + \frac{1}{2}\operatorname{erfc}\left\{\frac{THR_{GD}}{2\sigma_w^2\sqrt{2NM}}\right\}\right\}. \quad (54)$$

The case 4: $s_i^{\text{mod}}[k] = \mu s_i[k]$, $\mu \neq 1$, $\sigma_\zeta^2 \neq \sigma_\eta^2$, i.e., $\sigma_\zeta^2 = \sigma_w^2$ and $\sigma_\eta^2 = \beta\sigma_w^2$.

$$THR_{GD_{AWGN}}^{op} = \arg\min_{THR_{GD}} \frac{1}{2}\left\{1 - \frac{1}{2} \times \operatorname{erfc}\left\{\frac{THR_{GD} - NM\gamma\sigma_w^2(2\mu-1)}{\sigma_w^2\sqrt{2NM[(2\mu-1)^2\gamma^2 + 4(\mu-1)^2\gamma(1+\beta) + 2(1+\beta^2)]}}\right\} + \frac{1}{2}\operatorname{erfc}\left\{\frac{THR_{GD}}{2\sigma_w^2\sqrt{2NM(1+\beta^2)}}\right\}\right\}, \quad (55)$$

where [49]

$$Q(x) = \frac{1}{2}\operatorname{erfc}\left(\frac{x}{\sqrt{2}}\right) \quad (56)$$

is used to replace the Q-function with the complementary error function $\operatorname{erfc}(x)$. We determine the optimal threshold using the following equality

$$\frac{\partial[P_{error}^{GD}(THR_{GD})]}{\partial(THR_{GD})} = 0. \quad (57)$$

To solve (57) we can use the following equation [49]

$$\frac{\partial}{\partial x}\operatorname{erfc}\left(\frac{x-G}{L}\right) = -\frac{2}{L\sqrt{\pi}}\exp\left[-\frac{(x-G)^2}{L^2}\right], \quad (58)$$

where G and L are the arbitrary constants. Taking into consideration (52)–(58) we can write:

The case 1: $s_i^{\text{mod}}[k] = \mu s_i[k]$, $\mu = 1$, $\sigma_\zeta^2 = \sigma_\eta^2$.

$$\frac{\partial[P_{error}^{GD}(THR_{GD})]}{\partial(THR_{GD})} = \frac{1}{2}\left\{\frac{1}{\sqrt{2\pi NM(E_s^2\sigma_h^4 + 4\sigma_w^4)}}\exp\left\{-\frac{[THR_{GD} - NME_s\sigma_h^2]^2}{2NM(E_s^2\sigma_h^4 + 4\sigma_w^4)}\right\} - \frac{1}{2\sqrt{2\pi NM\sigma_w^4}}\exp\left\{-\frac{THR_{GD}^2}{8NM\sigma_w^4}\right\}\right\} = 0. \quad (59)$$

Solving (59) with respect to THR_{GD} (see Appendix 3), the GD optimal threshold in the case of the AWGN channel is defined in the following form:

$$THR_{GD_{AWGN}}^{op} \approx 2NM\sigma_w^2. \quad (60)$$

Thus, the optimal normalized GD threshold, the normalization factor is NM, defined as

$$\mathcal{THR}_{GD_{AWGN}}^{op} \approx \frac{THR_{GD_{AWGN}}^{op}}{NM} = 2\sigma_w^2 \quad (61)$$

is a function of the GD input noise variance only.

The case 2: $s_i^{\text{mod}}[k] = \mu s_i[k]$, $\mu = 1$, $\sigma_\xi^2 \neq \sigma_\eta^2$, i.e., $\sigma_\zeta^2 = \sigma_w^2$ and $\sigma_\eta^2 = \beta\sigma_w^2$.

$$\frac{\partial[P_{error}^{GD}(THR_{GD})]}{\partial(THR_{GD})} = \frac{1}{2}\left\{\frac{1}{\sqrt{2\pi NM[E_s^2\sigma_h^4 + 2\sigma_w^4(1+\beta^2)]}} \times \exp\left\{-\frac{[THR_{GD} - NME_s\sigma_h^2]^2}{2NM[E_s^2\sigma_h^4 + 2\sigma_w^4(1+\beta^2)]}\right\} - \frac{1}{2\sqrt{2\pi NM\sigma_w^4(1+\beta^2)}}\exp\left\{-\frac{THR_{GD}^2}{4NM\sigma_w^4(1+\beta^2)}\right\}\right\} = 0. \quad (62)$$

Solving (62) with respect to THR_{GD} (see Appendix 3), the GD optimal threshold in the case of the AWGN channel is defined in the following form:

$$THR_{GD_{AWGN}}^{op} \approx NM\sigma_w^2\sqrt{2(1+\beta^2)}. \quad (63)$$

The optimal normalized GD threshold is given by

$$\mathcal{THR}_{GD_{AWGN}}^{op} \approx \frac{THR_{GD_{AWGN}}^{op}}{NM} = \sigma_w^2\sqrt{2(1+\beta^2)}. \quad (64)$$

As follows from (64), if $\beta = 1$ we obtain the optimal GD detection threshold given in (60).

The case 3: $s_i^{\text{mod}}[k] = \mu s_i[k]$, $\mu \neq 1$, $\sigma_\zeta^2 = \sigma_\eta^2$.

$$\frac{\partial[P_{error}^{GD}(THR_{GD})]}{\partial(THR_{GD})} = \frac{1}{\sqrt{2\pi NM[(2\mu-1)^2E_s^2\sigma_h^4 + 4(\mu-1)^2E_s\sigma_h^2 + 4\sigma_w^4]}} \times \exp\left\{-\frac{[THR_{GD} - NM(2\mu-1)E_s\sigma_h^2]^2}{NM[(2\mu-1)^2E_s^2\sigma_h^4 + 4(\mu-1)^2E_s\sigma_h^2 + 4\sigma_w^4]}\right\} - \frac{1}{2\sigma_w^2\sqrt{2\pi NM}}\exp\left\{-\frac{THR_{GD}^2}{8NM\sigma_w^4}\right\} = 0. \quad (65)$$

Solving (65) with respect to THR_{GD} (see Appendix 3), the GD optimal threshold in the case of the AWGN channel is defined in the following form:

$$THR_{GD_{AWGN}}^{op} \approx 2(2\mu-1)NM\sigma_w^2. \quad (66)$$

The optimal normalized GD threshold is given by

$$\mathcal{THR}_{GD_{AWGN}}^{op} \approx \frac{THR_{GD_{AWGN}}^{op}}{NM} = 2(2\mu-1)\sigma_w^2. \quad (67)$$

The case 4: $s_i^{\text{mod}}[k] = \mu s_i[k]$, $\mu \neq 1$, $\sigma_\zeta^2 \neq \sigma_\eta^2$, i.e., $\sigma_\zeta^2 = \sigma_w^2$ and $\sigma_\eta^2 = \beta\sigma_w^2$.

$$\frac{\partial[P_{error}^{GD}(THR_{GD})]}{\partial(THR_{GD})} = \frac{1}{\sqrt{2\pi NM[(2\mu-1)^2E_s^2\sigma_h^4 + 2(\mu-1)^2E_s\sigma_h^2(1+\beta) + 2\sigma_w^4(1+\beta^2)]}} \times \exp\left\{-\frac{[THR_{GD} - NM(2\mu-1)E_s\sigma_h^2]^2}{2NM[(2\mu-1)^2E_s^2\sigma_h^4 + 2(\mu-1)^2E_s\sigma_h^2(1+\beta) + 2\sigma_w^4(1+\beta^2)]}\right\} - \frac{1}{2\sigma_w^2\sqrt{2\pi NM}}\exp\left\{-\frac{THR_{GD}^2}{4NM\sigma_w^4(1+\beta^2)}\right\} = 0. \quad (68)$$

Solving (68) with respect to THR_{GD} (see Appendix 2), the GD optimal threshold in the case of the AWGN channel is defined in the following form:

$$THR^{op}_{GD_{AWGN}} \approx \frac{2(2\mu-1)(1+\beta^2)}{(\mu-1)^2(1+\beta)} NM\sigma_w^2. \tag{69}$$

The optimal normalized GD threshold is given by

$$\mathcal{THR}^{op}_{GD_{AWGN}} \approx \frac{THR^{op}_{GD_{AWGN}}}{NM} = \frac{2(2\mu-1)(1+\beta^2)}{(\mu-1)^2(1+\beta)}\sigma_w^2. \tag{70}$$

As follows from (60), (63), (66), and (69) in the case of the AWGN channel, the GD optimal threshold is dependent on the noise power at the GD input, the relation between $s_i^{\text{mod}}[k]$ and $s_i[k]$, i.e., the value of μ, the value of β, the number of antenna array elements M, and the sample size N.

6.2. Nakagami-m fading channel

For a definition of the optimal GD threshold in the case of Nakagami-m fading channel there is a need to determine the average probability of miss $P^{GD_{av}}_{miss}$ and substitute it in the probability of error P^{GD}_{error} given by

$$P^{GD}_{error_{Nakagami}} = p_0 P^{GD}_{FA} + p_1 P^{GD_{av}}_{miss}. \tag{71}$$

Assume that the SNR distribution at the GD input is $p(\gamma)$. Then the average probability of $P^{GD_{av}}_{miss}$ can be presented in the following form:

$$P^{GD_{av}}_{miss} = \int_0^\infty P^{GD}_{miss}(\gamma)p(\gamma)d\gamma. \tag{72}$$

If the PU signal amplitude obeys the Nakagami-m distribution the SNR distribution $p(\gamma)$ at the GD input is [50]

$$p^{GD}_{Nakagami}(\gamma) = \frac{1}{\Gamma(m)}\left(\frac{m}{\gamma_{av}}\right)^m \gamma^{m-1}\exp\left\{-\frac{m}{\gamma_{av}}\gamma\right\}, \tag{73}$$

where γ_{av} is the average SNR at the GD input; m is the fading parameter, i.e., the parameter controlling the severity or depth of the amplitude fading; $\Gamma(m)$ is the Gamma function [50].

Considering the case 1, i.e., $s_i^{\text{mod}}[k] = \mu s_i[k]$, $\mu = 1$, $\sigma_\zeta^2 = \sigma_\eta^2$ the probability of miss P^{GD}_{miss} can be presented as

$$P^{GD}_{miss} = 1 - P^{GD}_{D} = 1 - \frac{1}{2}\operatorname{erfc}\left\{\frac{THR_{GD} - NM\gamma\sigma_w^2}{\sigma_w^2\sqrt{2NM(\gamma^2+4)}}\right\}. \tag{74}$$

Since CR systems operate at the low SNR, we can use the following approximation $\gamma^2 + 4 \approx 4$. Based on the equality

$$\frac{1}{2}\operatorname{erfc}(-x) = 1 - \frac{1}{2}\operatorname{erfc}(x) \tag{75}$$

(74) can be rewritten in the following form:

$$P^{GD}_{miss} = \frac{1}{2}\operatorname{erfc}\left\{\frac{NM\gamma\sigma_w^2 - THR_{GD}}{2\sigma_w^2\sqrt{2NM}}\right\}. \tag{76}$$

After substituting (73) and (76) in (72) we can write

$$P^{GD_{av}}_{miss_{Nakagami}} = \frac{1}{2\Gamma(m)}\left(\frac{m}{\gamma_{av}}\right)^m \int_0^\infty \gamma^{m-1}\exp\left\{-\frac{m}{\gamma_{av}}\gamma\right\} \times \operatorname{erfc}\left\{\frac{\gamma\sqrt{NM}}{2\sqrt{2}} - \frac{THR_{GD}}{2\sigma_w^2\sqrt{2NM}}\right\}d\gamma. \tag{77}$$

Taking into consideration the integral [51]

$$\int_0^\infty x^v \exp(-cx)\operatorname{erfc}(ax+b)dx = (-1)^v \frac{\partial^v}{dc^v}\left\{\frac{1}{c}\left[\operatorname{erfc}(b) - \exp\left\{-\frac{c^2+4abc}{4a^2}\right\}\operatorname{erfc}\left\{b+\frac{c}{2a}\right\}\right]\right\}, \tag{78}$$

where

$$v = m-1, m \text{ is integer}; a = \frac{\sqrt{NM}}{2\sqrt{2}}; b = -\frac{THR_{GD}}{2\sigma_w^2\sqrt{2NM}}; c = \frac{m}{\gamma_{av}}; \tag{79}$$

we can rewrite (77) in the following form:

$$P^{GD_{av}}_{miss_{Nakagami}} = (-1)^{m-1}\frac{1}{2\Gamma(m)}\left(\frac{m}{\gamma_{av}}\right)^m \frac{\partial^{m-1}}{\partial(m/\gamma_{av})^{m-1}} \times \left\{\frac{\gamma_{av}}{m}\left[\operatorname{erfc}\left\{-\frac{THR_{GD}}{2\sigma_w^2\sqrt{2NM}}\right\} - \exp\left\{-\frac{2m}{NM\gamma_{av}}\left[\frac{m}{\gamma_{av}} - \frac{THR_{GD}}{2\sigma_w^2}\right]\right\} \times \operatorname{erfc}\left\{\frac{m\sqrt{2}}{\gamma_{av}\sqrt{NM}} - \frac{THR_{GD}}{2\sigma_w^2\sqrt{2NM}}\right\}\right]\right\}. \tag{80}$$

Evidently, it is very difficult to derive the GD optimal threshold in the case of the Nakagami-m fading channel, especially if $m > 1$, because the probability of error

$$P^{GD}_{error_{Nakagami}} = p_0 P^{GD}_{FA} + p_1 P^{GD_{av}}_{miss_{Nakagami}} \tag{81}$$

has a nonlinear character. Thus, owing to $P^{GD}_{error_{Nakagami}}$ nonlinear character, as a result, a solution can be obtained numerically using MATLAB or other numerical methods and procedures.

6.3. Rayleigh fading channel

As before, we consider the case 1, i.e., $s_i^{\text{mod}}[k] = \mu s_i[k]$, $\mu = 1$, $\sigma_\zeta^2 = \sigma_\eta^2$. In the case of Rayleigh fading channel, the average probability of miss $P^{GD_{av}}_{miss_{Rayleigh}}$ can be obtained substituting $m = 1$ in (80), i.e., we can use the wide spread Rayleigh fading model:

$$P^{GD_{av}}_{miss_{Rayleigh}} = \frac{1}{2}\left\{\operatorname{erfc}\left\{-\frac{THR_{GD}}{2\sigma_w^2\sqrt{2NM}}\right\} - \exp\left\{-\frac{2}{NM\gamma_{av}}\left[\frac{1}{\gamma_{av}} - \frac{THR_{GD}}{2\sigma_w^2}\right]\right\} \times \operatorname{erfc}\left\{\frac{\sqrt{2}}{\gamma_{av}\sqrt{NM}} - \frac{THR_{GD}}{2\sigma_w^2\sqrt{2NM}}\right\}\right\}. \tag{82}$$

The case $m < 1$ corresponds to the high severe fading than the Rayleigh fading while the case $m > 1$ means the low severe fading in comparison with the Rayleigh fading [52]. The probability of error P^{GD}_{error} under the Rayleigh fading channel can be determined in the following form:

$$P^{GD}_{error_{Rayleigh}} = p_0 P^{GD}_{FA} + p_1 P^{GD_{av}}_{miss_{Rayleigh}}. \tag{83}$$

Table 1
The optimal thresholds of ED and GD.

	Fading channel type		
Detector	AWGN	Nakagami-m	Rayleigh
GD	$THR^{op}_{GD_{AWGN}} = 4NM\sigma_w^2$	$THR^{op}_{GD_{Nakagami}} = 4NM\sigma_w^2$	$THR^{op}_{GD_{Rayleigh}} = 4NM\sigma_w^2$
ED	$THR^{op}_{ED_{AWGN}} = NM\sigma_w^2$	$THR^{op}_{ED_{Nakagami}} = NM\sigma_w^2$	$THR^{op}_{ED_{Rayleigh}} = NM\sigma_w^2$

Based on the procedure discussed in the previous subsections there is a need to determine the first derivative of the probability of error $P^{GD}_{error_{Rayleigh}}$ given in (83) with respect to the detection threshold THR_{GD} to define the GD optimal threshold in the case of Rayleigh fading channel with the aid of (57), (58) [53] and (75). Thus, we obtain

$$\begin{aligned}\frac{\partial(P^{GD}_{error_{Rayleigh}})}{\partial(THR_{GD})} &= \frac{1}{2NM\gamma_{av}\sigma_w^2}\exp\left\{\frac{2}{NM\gamma_{av}}\left[\frac{1}{\gamma_{av}}-\frac{THR_{GD}}{2\sigma_w^2}\right]\right\} \\ &- \frac{1}{4\sqrt{2\pi NM}\gamma_{av}\sigma_w^2}\exp\left\{\frac{2}{NM\gamma_{av}}\left[\frac{1}{\gamma_{av}}-\frac{THR_{GD}}{2\sigma_w^2}\right]\right\} \\ &\times \exp\left\{-\frac{(\gamma_{av}THR_{GD}-4\sigma_w^2)^2}{8NM\gamma_{av}^2\sigma_w^4}\right\} \\ &- \frac{1}{4NM\gamma_{av}\sigma_w^2}\exp\left\{\frac{2}{NM\gamma_{av}}\left[\frac{1}{\gamma_{av}}-\frac{THR_{GD}}{2\sigma_w^2}\right]\right\} \\ &\times \operatorname{erfc}\left\{\frac{\gamma_{av}THR_{GD}-4\sigma_w^2}{2\sqrt{2NM}\gamma_{av}\sigma_w^2}\right\}. \end{aligned} \tag{84}$$

Setting (84) to zero and applying some mathematical transformations we obtain:

$$\exp\left\{-\frac{\gamma_{av}THR_{GD}-4\sigma_w^2}{2\sqrt{2NM}\gamma_{av}\sigma_w^2}\right\}\operatorname{erfc}\left\{\frac{\gamma_{av}THR_{GD}-4\sigma_w^2}{2\sqrt{2NM}\gamma_{av}\sigma_w^2}\right\} = \sqrt{\frac{NM}{2\pi}}\gamma_{av}. \tag{85}$$

Derivation of the direct formula of the optimal threshold $THR^{op}_{GD_{Rayleigh}}$ using (108) requires very cumbersome mathematics but it is possible to solve this problem applying numerical methods. Under the low SNR, $\gamma_{av} \ll 1$ the right side in (85) becomes negligible. Introduce the following notation:

$$\chi = -\frac{\gamma_{av}THR_{GD}-4\sigma_w^2}{2\sqrt{2NM}\gamma_{av}\sigma_w^2}. \tag{86}$$

In this case, we can write (85) as

$$\exp(-\chi^2)\operatorname{erfc}(\chi) = \sqrt{\frac{NM}{2\pi}}\gamma_{av}. \tag{87}$$

We can notice that if $\gamma_{av} \ll 1$ and $THR_{GD} \to 4NM\sigma_w^2$ the left side in (87) tends to approach a very small value:

$$\lim_{\chi\to\infty}\exp(-\chi^2)\operatorname{erfc}(\chi) \to 0. \tag{88}$$

Based on (87) and (88) we see that the optimal GD detection threshold is approximately closed to $4NM\sigma_w^2$. Thus, in the case of Rayleigh fading channel, the optimal GD threshold can be approximated by the following form:

$$THR^{op}_{GD_{Nakagami}} \approx 4NM\sigma_w^2. \tag{89}$$

Owing to the fact that the Nakagami-m fading varies between the Rayleigh fading and Gaussian fading, $1 < m < \infty$, the optimal GD threshold in the case of Nakagami-m fading channel is also close to $4NM\sigma_w^2$:

$$THR^{op}_{GD_{Nakagami}} \approx 4NM\sigma_w^2. \tag{90}$$

As follows from (89) and (90), the normalized GD optimal threshold with the normalization factor NM in the case of Rayleigh and Nakagami-m fading channels can be defined as:

$$\mathcal{THR}^{op}_{GD_{Rayleigh}} = \mathcal{THR}^{op}_{GD_{Nakagami}} \approx \frac{THR^{op}_{GD_{Rayleigh}}}{NM} = 4\sigma_w^2. \tag{91}$$

Applying the same procedure for the conventional ED with the purpose to define the optimal detection threshold we can find that the ED optimal threshold is approximately the same under all fading channels as shown in [54]:

$$THR^{op}_{GD_{AWGN}} = THR^{op}_{GD_{Rayleigh}} = THR^{op}_{GD_{Nakagami}} \approx NM\sigma_w^2. \tag{92}$$

A brief summary of the analysis of Section 6 is presented in Table 1 and Table 2. In Table 1 we present the optimal ED and GD thresholds under various channel types and for the ideal initial condition in the case of GD, $\mu = 1$, $\beta = 1$. Table 2 is dedicated to the GD presenting the ideal and non-ideal conditions and the related optimal threshold for each case under the AWGN channel.

Table 2
The optimal thresholds of GD in the case of AWGN channel under ideal and non-ideal conditions.

The case	Optimal threshold
$\mu = 1$ and $\beta = 1$	$(THR^{op}_{GD})_{AWGN} = 2NM\sigma_w^2$
$\mu = 1$ and $\beta \neq 1$	$(THR^{op}_{GD})_{AWGN} = NM\sigma_w^2\sqrt{2(1+\beta^2)}$
$\mu \neq 1$ and $\beta = 1$	$(THR^{op}_{GD})_{AWGN} = 2(2\mu-1)NM\sigma_w^2$
$\mu \neq 1$ and $\beta \neq 1$	$(THR^{op}_{GD})_{AWGN} \approx \frac{2(2\mu-1)(1+\beta^2)}{(\mu-1)^2(1+\beta)}NM\sigma_w^2$

7. Simulation results

In this section, we verify the spectrum sensing performance of the conventional GD and the proposed WGD and GLRT-GD by simulation using MATLAB and compare it with other detectors under the uncorrelated and correlated antenna array elements. Simulation is performed using IEEE 802.22 system parameters [54]. The main simulation parameters are presented in Table 3.

Comparison of the spectrum sensing performance between the conventional GD, conventional ED, MF, and GLRT detector proposed in [13] under assumption that the noise power is known is presented in Fig. 3 when the number of antenna array elements is equal to 6, $M = 6$, the number of samples is equal to 20, $N = 20$, and the antenna array elements are independent, i.e., $\rho = 0$. The test statistics at the GLRT detector output suggested in [13] has a simple form of the ratio between the largest eigenvalue and the sum of eigenvalues of the sample covariance matrix of the incoming PU signal. As shown in Fig. 3, the conventional GD demonstrates the better performance in comparison with other above-mentioned detectors. For example, the conventional GD achieves 3 dB SNR gain in comparison with the conventional ED at the probability of false alarm P_{FA} equal to 0.5; the SNR gain is equal approximately to 1 dB in favor of the conventional GD comparing

Table 3
Main simulation parameters.

Parameter	Value
The angular spread (correlated antenna array elements)	$\Delta = 0.5°$
The angular spread (uncorrelated antenna array elements)	$\Delta = 180°$
Distance between antenna elements (correlated antenna array elements)	$d = \lambda/8$
Distance between antenna elements (uncorrelated antenna array elements)	$d = \lambda/2$
Number of antenna array elements	M is varied from 2 to 10
SNR	γ is varied from −20 dB to 0 dB
P_D constraint	$\alpha = 0.99$
Coefficient of correlation	$\rho = 0; 0.1; 0.25; 0.5; 0.75; 0.9; 1.0$
Channel parameter	$\sigma_h^2 = 1$
Number of samples	$N = 20; 100$

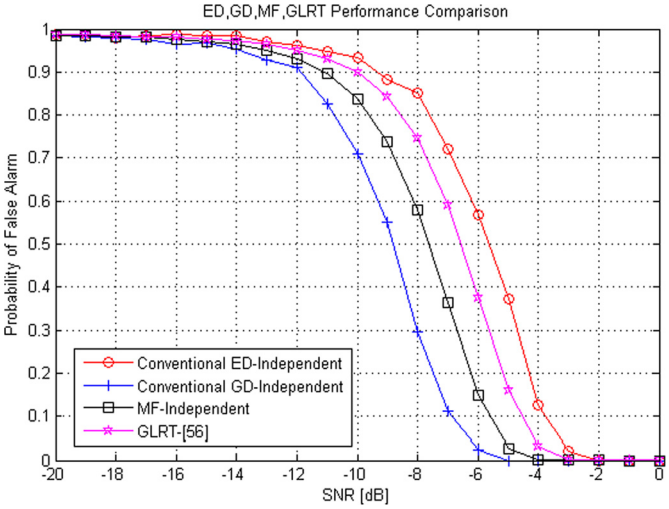

Fig. 3. Comparison of spectrum sensing performance between the conventional ED, GD, MF, and GLRT [56] detectors under the independent antenna array elements.

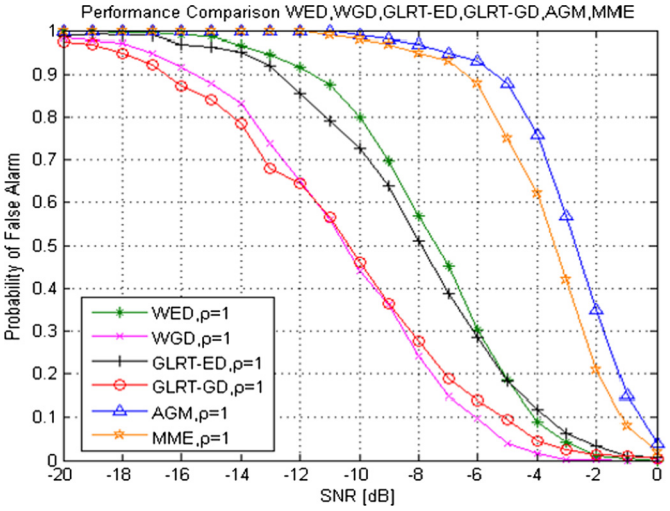

Fig. 4. Comparison of spectrum sensing performance between the WED, WGD, GLRT-ED, GLRT-GD, MME and AGM detectors under the correlated antenna array elements.

with the MF; and the SNR gain is about 2 dB in comparison with the GLRT detector proposed in [13].

In Fig. 4 the spectrum sensing performances of the WED, WGD, GLRT-ED, GLRT-GD, AGM, and MME detectors are compared between each other in the case when the antenna array elements are correlated, $\rho = 1$, the number of antenna array elements is equal to 6, $M = 6$, the number of samples is equal to 20, $N = 20$. The GLRT-GD and WGD have very close spectrum sensing performance. The GLRT-GD achieves the SNR gain equal to 2.5 dB, 6.5 dB, and 7 dB in comparison with GLRT-ED, MME, and AGM detectors, respectively at the probability of false alarm $P_{FA} = 0.5$.

In the case of the uncorrelated antenna array elements, the WGD and WED are just the conventional GD and conventional ED, respectively. We can notice from Figs. 3 and 4 that in the case of the correlated antenna array elements, the spectrum sensing performance both for ED and GD is worse, i.e., the probability of false alarm P_{FA} is high, in comparison with the case of the uncorrelated antenna array elements. The proposed WGD and GLRT-GD allow us to improve the spectrum sensing performance in comparison with the conventional GD when the antenna array elements are correlated.

Effect of the coefficient of correlation ρ on the spectrum sensing performance of WED, WGD, GLRT-ED, GLRT-GD is presented in Fig. 5 at $M = 6$, $N = 20$, $\rho = 0.5; 1.0$. As we can see from Fig. 5, the probability of false alarm P_{FA} is increased with increasing in the correlation coefficient ρ from 0.5 to 1.0 for all detectors. These results confirm a negative action of the coefficient of correlation ρ between the adjacent antenna array elements on detection performance.

The receiver operation characteristic (ROC) curves for the GD, ED, WED, WGD, GLRT-ED, GLRT-GD are presented in Fig. 6 when

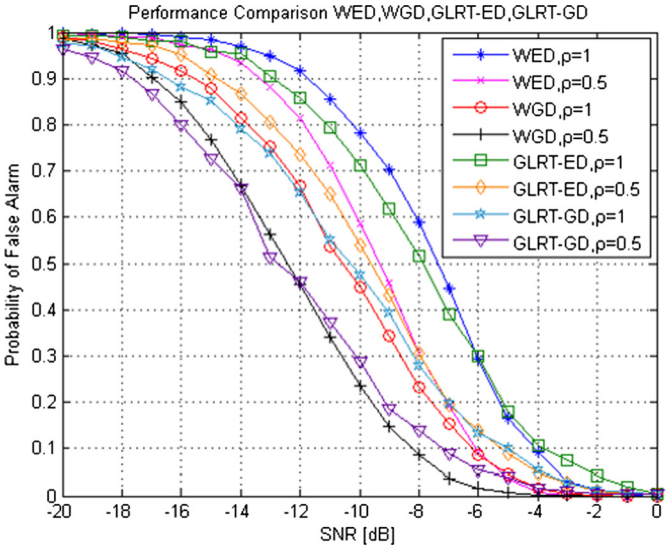

Fig. 5. Comparison of spectrum sensing performance between the WED, WGD, GLRT-ED, and GLRT-GD under different values of the coefficient of correlation.

the antenna array elements are spatially correlated $\rho = 1.0$ at $M = 6$, $N = 20$ and $SNR = -10$ dB. The WGD and GLRT-GD demonstrate superiority in sensing performance in comparison with the WED and GLRT-ED For example, at the probability of false alarm $P_{FA} = 0.1$ in the case of WED and GLRT-ED, the probability of detection P_D is equal to 0.55 and 0.6, respectively, while in the case

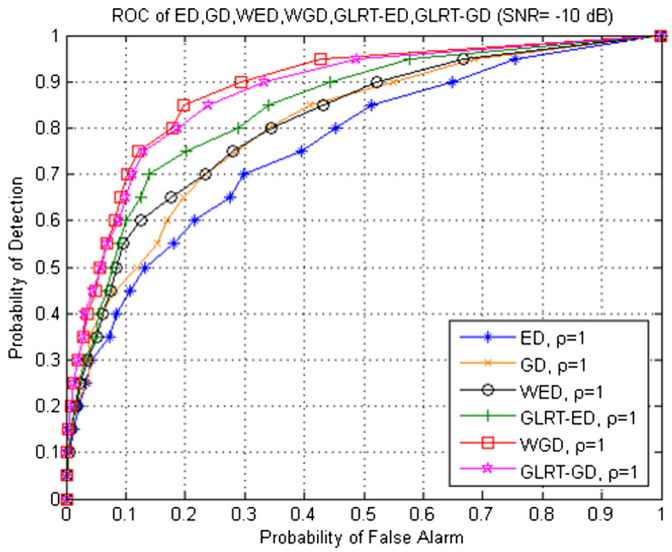

Fig. 6. ROC curves of ED, GD, WED, WGD, GLRT-ED, and GLRT-GD under correlated antenna array elements ($\rho = 1$) at $SNR = -10$ dB.

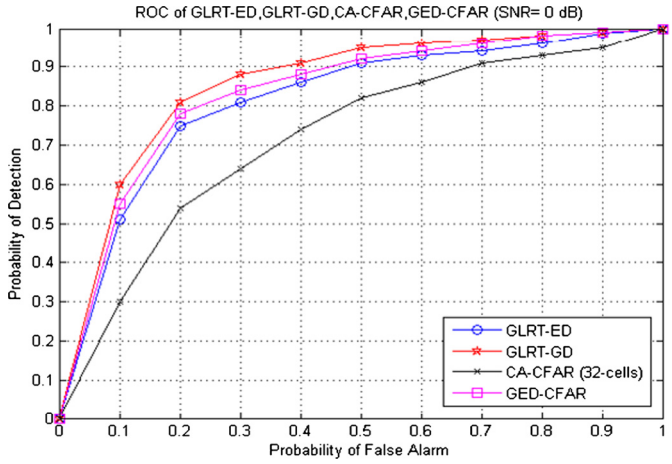

Fig. 7. ROC curves of GLRT-ED, GLRT-GD, CA-CFAR, and GED-CFAR detectors at $SNR = 0$ dB.

of WGD the probability of detection P_D is approximately equal to 0.7, the same as in the case of the GLRT-GD.

In Fig. 7 the ROC curves of constant detection rate (CDR) algorithms, namely, the proposed GLRT-GD and GLRT-ED, and the constant false alarm rate (CFAR) algorithms presented by the cell averaging CFAR, CA-CFAR with 32 reference cells, and the generalized ED with CFAR property, GED-CFAR [39] (the analysis in detail is presented in [40]) are shown at $M = 6$, $N = 20$ and $SNR = 0$ dB. All these detectors share the presence of noise power estimation techniques. The GLRT-GD demonstrates the best performance among other detectors and closely followed by the GED-CFAR performance.

In Fig. 8, the performance of new signal detection algorithms is compared with the performance ROC of CBD [10], EME [12], SLE [13], MBD [14], and max-min SNR detectors at $M = 6$, $N = 20, 100$, and $SNR = -10$ dB. As presented in Fig. 8, the WGD has the best performance in comparison with all other detectors. In fact, the max-min SNR detector performs slightly better than the WGD in the region when its probability of false alarm P_{FA} is within the limits of the interval $[0, 0.15]$, but it is noticeable that the number of samples N is less in the case of WGD. Thus, the GD and GLRT-GD have the better performance under small number of samples $N = 20$ comparing with the EME, CBD, MBD, and max-min

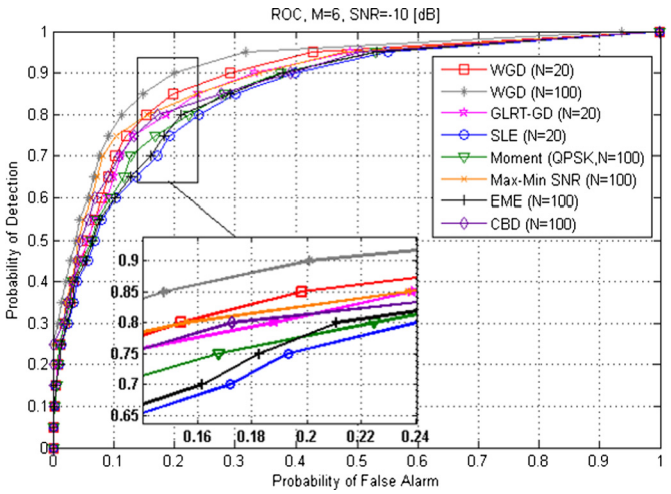

Fig. 8. ROC curves of WGD, GLRT-GD, SLE, EME, CBD, moment detector, and max-min SNR detector under correlated antenna array elements ($\rho = 1$) at $SNR = -10$ dB.

SNR detectors where their performances are shown under very big number of samples in the related references [10,12,14], and [15], respectively. The SLE detector shares with WGD and GLRT-GD the ability to perform well under small sample size $N = 20$. All detectors shown in Fig. 8 benefit from the large sample size and they have very closed performances if the sample size is, for instance $N = 100$.

Comparison of the spectrum sensing performance in terms of the probability of error P_{error} between the conventional GD and ED when the antenna array elements are uncorrelated is presented in Fig. 9 for various fading channels, namely, the AWGN, Nakagami-2, and Rayleigh channels at the ideal operating conditions for the GD, i.e., $\mu = 1$, $\beta = 1$. These results are obtained at $M = 2$, $N = 100$ and $SNR = -5$ dB. The probability of error P_{error} is evaluated for both detectors as a function of the normalized optimal detection threshold with the normalization factor equal to NM. As follows from Fig. 9, the conventional GD can achieve the low probability of error P_{error} in comparison with the conventional ED for all above-mentioned fading channels at the same SNR. For example, in the case of the AWGN fading channel, the lowest probability of error P_{error}^{GD} is equal to 0.19, while the lowest probability of error P_{error}^{ED} is equal to 0.45.

In Fig. 10 the probability of error P_{error}^{GD} is evaluated at the non-ideal operating conditions of the conventional GD, i.e., $\mu \neq 1$ and $\beta \neq 1$, the noise variance or power at the GD AF and GD PF outputs is differed, and compared with the probability of error P_{error}^{GD} at $M = 2$, $N = 100$ and $SNR = -5$ dB. Evidently, the P_{error}^{GD} performance is deteriorated in the case $\beta \neq 1$ in comparison with $\beta = 1$. This performance degradation is the direct negative effect caused by the inequality between the noise variance or noise power at the GD PF and GD AF outputs. As shown in Fig. 10, the conventional GD presents the better P_{error} performance in comparison with the conventional ED even under the non-ideal operating conditions.

In Fig. 11 the P_{error}^{GD} performance is presented under the following operating conditions $\mu = 1$, $\beta \neq 1$ and $\mu \neq 1$, $\beta \neq 1$ of the conventional GD at $M = 2$, $N = 100$ and $SNR = -5$ dB. As follows from Fig. 10, the P_{error}^{GD} performance degradation caused by the non-ideal operating conditions is apparent in comparison with the ideal case $\mu = 1$, $\beta = 1$. This P_{error}^{GD} performance deterioration is a function of the factors μ and β. The conventional GD demonstrates robustness against the non-ideal conditions and presents in the most cases the better probability of error performance comparing with the conventional ED (Fig. 9 and Fig. 10). At $\mu = 0.6$, $\beta = 0.6$ (see Fig. 11), the conventional ED demonstrates the better

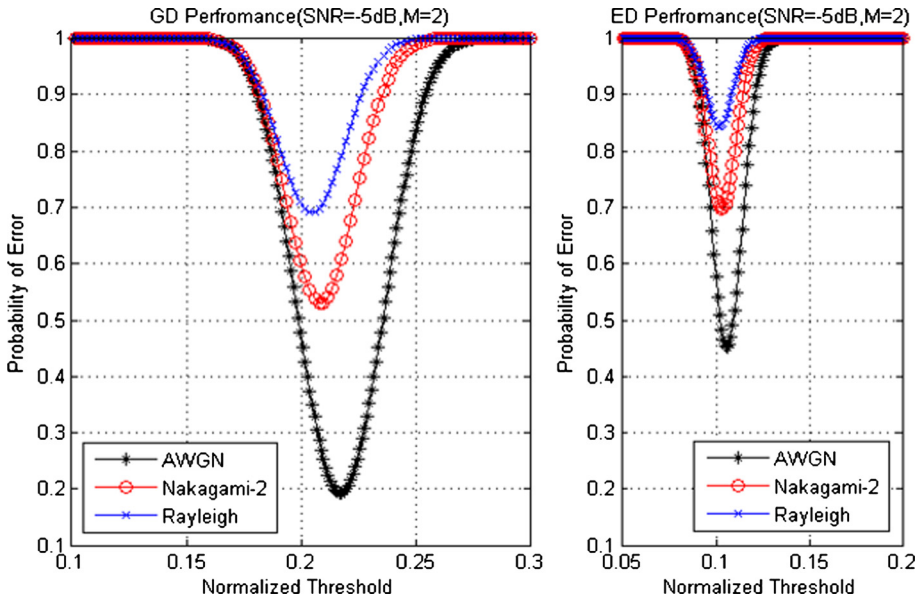

Fig. 9. Probability of error P_{error} for the conventional ED and GD (ideal functioning case $\mu = 1$ and $\beta = 1$) as a function of the normalized threshold over AWGN, Nakagami-2, and Rayleigh fading channels.

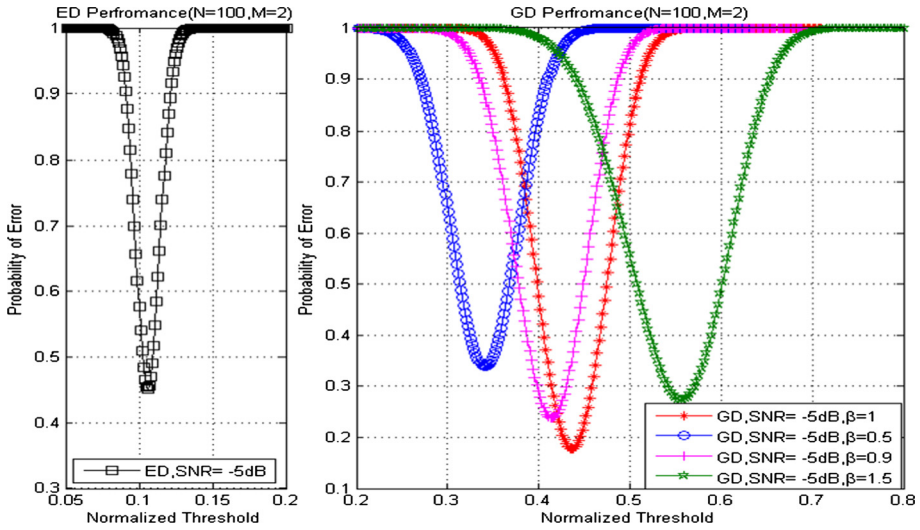

Fig. 10. Probability of error P_{error} for the conventional ED and GD (non-ideal operating conditions $\mu = 1$ and $\beta \neq 1$) as a function of the normalized threshold over AWGN fading channel.

probability of error performance in comparison with the conventional GD (see Fig. 10 and Fig. 11).

The performance of new detectors, namely, WGD and GLRT-GD in the form of the complementary receiver operation characteristic (CROC) is presented in Fig. 12 under the noise uncertainty when the noise power can be defined within the limits of the specific interval $\sigma_w^2 \in [\delta^{-1}\sigma^2, \delta\sigma^2]$, where σ^2 is the nominal noise power at the GD input [55,56] and δ is the uncertainty parameter given by

$$\delta = 10^{0.1\varepsilon}, \tag{93}$$

where ε is the parameter used to define the amount of non-probabilistic uncertainty in the noise power. The results in Fig. 12 are obtained at $M = 6$, $N = 20$ and $SNR = -10, -15$ dB and $\varepsilon = 1$ dB. As follows from Fig. 12, the noise power uncertainty has a negative effect on the CROC performance of the conventional GD and WGD and GLRT-GD as well. In general, the WGD and GLRT-GD improve the conventional GD immunity against the noise power uncertainty and the GLRT-GD has the better CROC performance in comparison with the WGD. More details about the conventional GD character under the noise power uncertainty can be found in [41].

Modifications of the conventional GD, namely, the WGD and GLRT-GD require more computational cost in comparison with the conventional GD owing to a need to compute eigenvalues of the correlation and sample covariance matrices both in the case of the WED and GLRT-GD. Evaluation and comparison of the GD computational cost with other detectors is outside a scope of the present paper.

8. Conclusions

The spectrum sensing in the CR networks requires sensors that are able to detect the frequency holes in a reliable, robust, and computationally feasible manner. By these reasons, we suggest to employ the GD with the purpose to improve the spectrum sensing performance. Comparison of the conventional ED and GD spectrum sensing performances is carried out at the same initial conditions

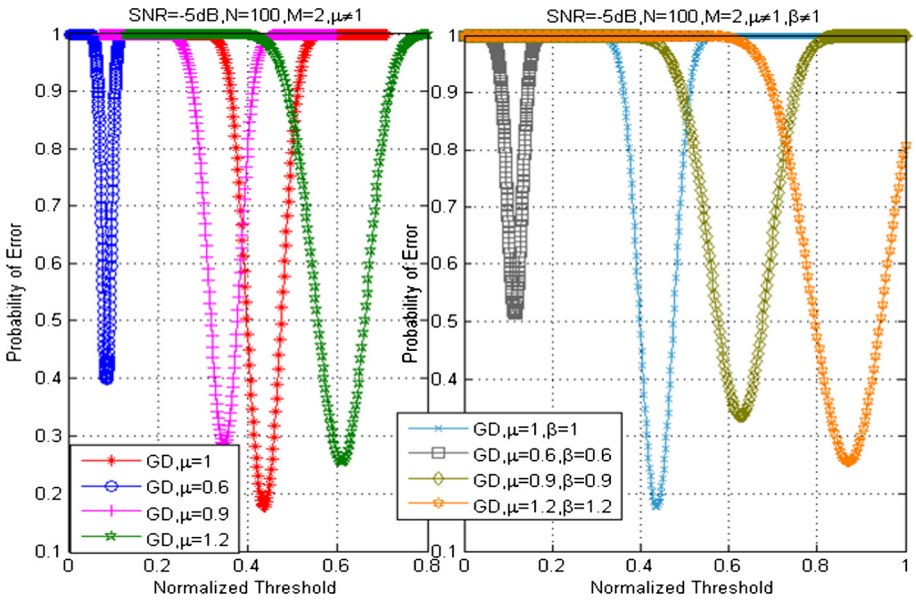

Fig. 11. The P_{error} as a function of the normalized threshold over AWGN fading channel under extreme non-ideal operating conditions for GD, $\mu \neq 1$ and $\beta \neq 1$.

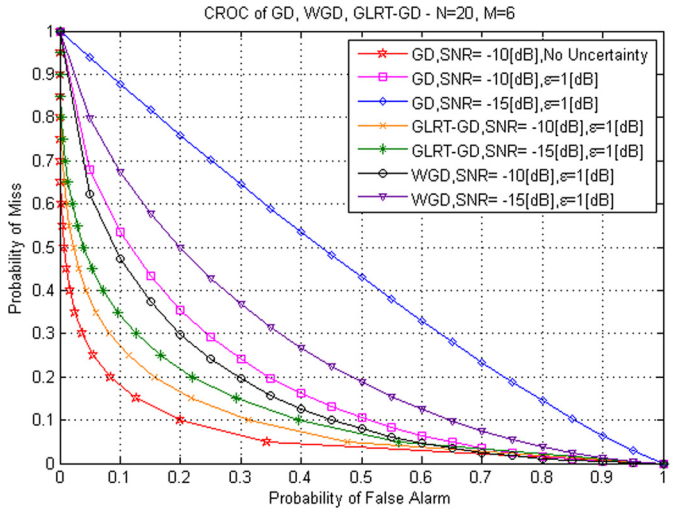

Fig. 12. Complementary ROC of the conventional GD, WGD, and GLRT-GD under noise power uncertainty.

under the uncorrelated and spatially correlated antenna array elements. The conventional GD demonstrates the better sensing performance in comparison with the conventional ED both under the uncorrelated and correlated antenna array elements.

To improve further the spectrum sensing performance under the correlated antenna array elements, the WGD is suggested in the case if the noise power is known and GLRT-GD is proposed in the case when the noise power is unknown. The simulation results demonstrate validity and superiority of the WGD and GLRT-GD implementation in CR systems in comparison with the WED, GLRT-ED, MME, AGM, EME, CBD, SLE, MBD, and max-min SNR detectors.

The conventional GD and its modifications can deliver the low probability of error in comparison with the conventional ED at the same SNR in the case of the AWGN, Nakagami-*m*, and Rayleigh fading channels using the optimal detection threshold defined for each type of fading channels applying the minimum probability of error criterion. The negative effects of the non-ideal conditions, namely, the coefficient of proportionality is not unity and the noise power at the GD PF and AF outputs are not identical, on the GD performance are evaluated. The GD demonstrates robustness against the non-ideal conditions and maintains a considerable spectrum sensing performance improvement.

Declaration of competing interest

There is no any conflict of interests between the authors.

Acknowledgments

This research has been supported by the National Council of Science and Technology in Mexico (Censejo Nacional Ciencia y Tecnology – CONACYT, research grant no 35022). Additionally, the authors would like to thank the anonymous reviewers for the comments and suggestions that helped to improve a quality of the present paper.

Appendix 1

WGD. According to the GASP, the GD likelihood functions under the hypotheses $\mathcal{H}_1$ and $\mathcal{H}_0$ can be presented in the following form:

$$p\left(\boldsymbol{\eta}|\mathcal{H}_0,\sigma_w^2\right)=\prod_{k=0}^{N-1}\frac{1}{\sqrt{(2\pi\sigma_w^2\mathbf{I})^M}}\exp\left\{-\frac{\boldsymbol{\eta}^H[k]\boldsymbol{\eta}[k]}{2\sigma_w^2\mathbf{I}}\right\}, \tag{94}$$

$$p\left(\mathbf{X}|\mathcal{H}_1,\sigma_w^2\right)=\prod_{k=0}^{N-1}\frac{1}{\sqrt{(2\pi)^M\det(E_s\sigma_h^2\mathbf{R}+\sigma_w^2\mathbf{I})}}\times\exp\left\{-\frac{\mathbf{X}^H[k]\mathbf{X}[k]}{2(E_s\sigma_h^2\mathbf{R}+\sigma_w^2\mathbf{I})}\right\}, \tag{95}$$

where $\boldsymbol{\eta}=\{\boldsymbol{\eta}[0],\ldots,\boldsymbol{\eta}[N-1]\}$ and $\boldsymbol{\eta}[k]$, $k=0,\ldots,N-1$ is the $M\times 1$ vector of the k-th sample of the reference noise or secondary data at the GD AF output; H denotes the Hermitian conjugate; and $\det(\cdot)$ is the determinant of the matrix. Based on the Neyman-Pearson theorem when the noise variance σ_w^2 is known the GD decision statistics can be obtained based on the LRT as follows:

$$L_{GD}(\mathbf{X})=\frac{p(\mathbf{X}|\mathcal{H}_1,\sigma_w^2)}{p(\boldsymbol{\eta}|\mathcal{H}_0,\sigma_w^2)}$$

$$= \prod_{k=0}^{N-1} \sqrt{\frac{\sigma_w^{2M}}{\det(E_s\sigma_h^2\mathbf{R}+\sigma_w^2\mathbf{I})}} \times \exp\left\{-\frac{\mathbf{X}^H[k]\mathbf{X}[k]}{2(E_s\sigma_h^2\mathbf{R}+\sigma_w^2\mathbf{I})}+\frac{\boldsymbol{\eta}^H[k]\boldsymbol{\eta}[k]}{2\sigma_w^2\mathbf{I}}\right\}. \quad (96)$$

After taking the logarithm of (96) and retaining the data dependent terms only, we can define the GD log-LRT using the following form:

$$\ln L_{GD}(\mathbf{X}) = -\sum_{k=0}^{N-1}\frac{\mathbf{X}^H[k]\mathbf{X}[k]}{2(E_s\sigma_h^2\mathbf{R}+\sigma_w^2\mathbf{I})}+\sum_{k=0}^{N-1}\frac{\boldsymbol{\eta}^H[k]\boldsymbol{\eta}[k]}{2\sigma_w^2\mathbf{I}}. \quad (97)$$

Using the matrix inversion lemma [3]

$$(\mathbf{A}+\mathbf{BFD})^{-1} = \mathbf{A}^{-1}-\mathbf{A}^{-1}\mathbf{B}\big(\mathbf{DA}^{-1}\mathbf{B}+\mathbf{F}^{-1}\big)^{-1}\mathbf{DA}^{-1} \quad (98)$$

and letting $\mathbf{A}=\sigma_w^2\mathbf{I}$, $\mathbf{B}=\mathbf{D}=\mathbf{I}$, and $\mathbf{F}=E_s\sigma_h^2\mathbf{R}$ we obtain

$$\begin{aligned}&\big(E_s\sigma_h^2\mathbf{R}+\sigma_w^2\mathbf{I}\big)^{-1}\\ &= \frac{1}{\sigma_w^2}\mathbf{I}-\frac{1}{\sigma_w^4}\left[\frac{1}{\sigma_w^2}\mathbf{I}+\frac{1}{E_s\sigma_h^2}\mathbf{R}^{-1}\right]^{-1}\\ &= \frac{1}{\sigma_w^2}\Bigg\{\mathbf{I}-\underbrace{\frac{1}{\sigma_w^2}\left[\frac{1}{\sigma_w^2}\mathbf{I}+\frac{1}{E_s\sigma_h^2}\mathbf{R}^{-1}\right]^{-1}}_{Z}\Bigg\}.\end{aligned} \quad (99)$$

Introduce the term $\mathcal{Z}$ in (99)

$$\begin{aligned}\mathcal{Z} &= \frac{1}{\sigma_w^2}\left[\frac{1}{\sigma_w^2}\mathbf{I}+\frac{1}{E_s\sigma_h^2}\mathbf{R}^{-1}\right]^{-1}\\ &= \frac{1}{\sigma_w^2}\left[\frac{1}{E_s\sigma_h^2\sigma_w^2}\big(E_s\sigma_h^2\mathbf{R}+\sigma_w^2\mathbf{I}\big)\mathbf{R}^{-1}\right]^{-1}\\ &= E_s\sigma_h^2\mathbf{R}\big(E_s\sigma_h^2\mathbf{R}+\sigma_w^2\mathbf{I}\big)^{-1}.\end{aligned} \quad (100)$$

Using (99) and (100), (97) can be written in the following form:

$$\begin{aligned}&\ln L_{GD}(\mathbf{X})\\ &= \frac{1}{2\sigma_w^2}\Bigg\{\sum_{k=0}^{N-1}\mathbf{X}^H[k]\big[E_s\sigma_h^2\mathbf{R}\big(E_s\sigma_h^2\mathbf{R}+\sigma_w^2\mathbf{I}\big)^{-1}-\mathbf{I}\big]\mathbf{X}[k]\\ &\quad+\sum_{k=0}^{N-1}\boldsymbol{\eta}^H[k]\boldsymbol{\eta}[k]\Bigg\}\\ &= \frac{1}{2\sigma_w^2}\Bigg\{\sum_{k=0}^{N-1}\mathbf{X}^H[k]\big[E_s\sigma_h^2\mathbf{R}\big(E_s\sigma_h^2\mathbf{R}+\sigma_w^2\mathbf{I}\big)^{-1}+\sigma_w^2\mathbf{I}\big]\mathbf{X}[k]\\ &\quad-\sum_{k=0}^{N-1}\mathbf{X}^H[k]\mathbf{X}[k]+\sum_{k=0}^{N-1}\boldsymbol{\eta}^H[k]\boldsymbol{\eta}[k]\Bigg\}.\end{aligned} \quad (101)$$

To perform the eigendecomposition on the matrix $\mathbf{R}$, let us define $\mathbf{Y}[k]=\mathbf{V}^H\mathbf{X}[k]$, where $\mathbf{V}=[\mathbf{v}_0,\ldots,\mathbf{v}_{N-1}]$ with the $\mathbf{v}_i$ eigenvector of the matrix $\mathbf{R}$. Since the matrix $\mathbf{V}$ is orthogonal, then $\mathbf{V}^H=\mathbf{V}^{-1}$. The decorrelation matrix $\mathbf{V}$ is the modal matrix for the symmetric matrix $\mathbf{R}$. The first term in (101) can be presented in the following form

$$\begin{aligned}&\frac{1}{2\sigma_w^2}\sum_{k=0}^{N-1}\mathbf{X}^H[k]\big[E_s\sigma_h^2\mathbf{R}\big(E_s\sigma_h^2\mathbf{R}+\sigma_w^2\mathbf{I}\big)^{-1}\big]\mathbf{X}[k]\\ &= \frac{E_s\sigma_h^2}{2\sigma_w^2}\sum_{k=0}^{N-1}\mathbf{X}^H[k]\mathbf{V}\mathbf{V}^H[\mathbf{RV}\mathbf{V}^{-1}\big(E_s\sigma_h^2\mathbf{R}+\sigma_w^2\mathbf{I}\big)^{-1}\mathbf{V}\mathbf{V}^H\mathbf{X}[k]\\ &= \frac{E_s\sigma_h^2}{2\sigma_w^2}\sum_{k=0}^{N-1}\big[\mathbf{V}^H\mathbf{X}[k]\big]^H\big(\mathbf{V}^H\mathbf{RV}\big)\big[\mathbf{V}^{-1}\big(E_s\sigma_h^2\mathbf{R}+\sigma_w^2\mathbf{I}\big)\mathbf{V}\big]^{-1}\mathbf{V}^H\mathbf{X}[k]\\ &= \frac{E_s\sigma_h^2}{2\sigma_w^2}\sum_{k=0}^{N-1}\big[\mathbf{V}^H\mathbf{X}[k]\big]^H\big(\mathbf{V}^H\mathbf{RV}\big)\big(E_s\sigma_h^2\mathbf{V}^H\mathbf{RV}+\sigma_w^2\mathbf{I}\big)^{-1}\mathbf{V}^H\mathbf{X}[k].\end{aligned} \quad (102)$$

Now we have that $\mathbf{V}^H\mathbf{RV}=\boldsymbol{\Lambda}$, where $\boldsymbol{\Lambda}=diag(\alpha_0,\ldots,\alpha_{N-1})$ is the diagonal matrix with the α_i eigenvalues of the correlation matrix $\mathbf{R}$. Thus, we can rewrite (102) as follows:

$$\begin{aligned}&\frac{E_s\sigma_h^2}{2\sigma_w^2}\mathbf{X}^H[k]\big[\mathbf{R}\big(E_s\sigma_h^2\mathbf{R}+\sigma_w^2\mathbf{I}\big)^{-1}\big]\mathbf{X}[k]\\ &= \frac{E_s\sigma_h^2}{2\sigma_w^2}\sum_{k=0}^{N-1}\mathbf{Y}^H[k]\boldsymbol{\Lambda}\big(E_s\sigma_h^2\boldsymbol{\Lambda}+\sigma_w^2\mathbf{I}\big)^{-1}\mathbf{Y}[k].\end{aligned} \quad (103)$$

The second term in (101) can be presented as

$$\frac{1}{2\sigma_w^2}\sum_{k=0}^{N-1}\mathbf{X}^H[k]\mathbf{X}[k] = \frac{N}{2\sigma_w^2}\sum_{i=1}^{M}\lambda_{R_x i}, \quad (104)$$

where $\lambda_{R_x i}$ is the i-th eigenvalue of the sample covariance matrix $\mathbf{R}_{\boldsymbol{\eta}}$ of the observed sample $\boldsymbol{\eta}$ given by

$$\mathbf{R}_{\boldsymbol{\eta}} = N^{-1}\boldsymbol{\eta}\boldsymbol{\eta}^H. \quad (105)$$

GLRT-GD. In the case of unknown parameters of the noise, we can replace these parameters by their maximum likelihood estimates (MLE) under each hypothesis [3]. If the noise variance σ_w^2 is unknown, we apply the GLRT-GD and obtain the MLE of the noise variance σ_w^2 under consideration of the hypotheses $\mathcal{H}_0$ and $\mathcal{H}_1$, correspondingly. Thus, the GLRT-GD test can be presented using the following form:

$$L_{GD}^{GLRT}(\mathbf{X}) = \frac{p(\mathbf{X}|\mathcal{H}_1,\hat{\sigma}_1^2)}{p(\mathbf{X}|\mathcal{H}_0,\hat{\sigma}_0^2)}, \quad (106)$$

where $\hat{\sigma}_0^2$ is the MLE of the noise variance σ_w^2 under the hypothesis $\mathcal{H}_0$ and $\hat{\sigma}_1^2$ is the MLE of the GD total noise component variance under the hypothesis $\mathcal{H}_1$. The PU signal has stochastic parameters owing to fading channels.

To define the MLE $\hat{\sigma}_0^2$ we take the logarithm of (94) to get the log-likelihood function as follows:

$$\ln p(\boldsymbol{\eta}|\mathcal{H}_0) = -0.5NM\ln 2\pi\sigma_w^2-\frac{1}{2\sigma_w^2}\sum_{k=0}^{N-1}\boldsymbol{\eta}^H[k]\boldsymbol{\eta}[k]\mathbf{I}. \quad (107)$$

The MLE $\hat{\sigma}_0^2$ is obtained solving the following equation [3]:

$$\frac{\partial}{\partial\sigma_w^2}\ln p(\boldsymbol{\eta}|\mathcal{H}_0) = -\frac{1}{2\sigma_w^2}\left[NM-\sum_{k=0}^{N-1}\boldsymbol{\eta}^H[k]\boldsymbol{\eta}[k]\mathbf{I}\right] = 0. \quad (108)$$

Solution of (108) with respect to σ_w^2 gives us

$$\hat{\sigma}_0^2 = \frac{1}{NM}\sum_{k=0}^{N-1}\boldsymbol{\eta}^H[k]\boldsymbol{\eta}[k]\mathbf{I} = \frac{1}{M}\sum_{i=1}^{M}\lambda_{R_\eta i}. \quad (109)$$

We should apply the same procedure to find the MLE $\hat{\sigma}_1^2$ of the GD total noise component variance under the hypothesis $\mathcal{H}_1$. Taking the logarithm of (95) we obtain

$$\ln p\big(\mathbf{Y}=\mathbf{V}^H\mathbf{X}|\mathcal{H}_1\big) = -\frac{NM}{2}\ln\pi - \frac{N}{2}\sum_{i=1}^{M}\ln\big(E_s\sigma_h^2\alpha_i+\sigma_w^2\big) - \sum_{k=0}^{N-1}\sum_{i=1}^{M}\frac{\{\mathbf{V}_i^H\mathbf{X}[k]\}^2}{(E_s\sigma_h^2\alpha_i+\sigma_w^2)}. \tag{110}$$

Taking the first derivative of (110) with respect to σ_w^2 and setting it to zero we obtain the following equation

$$\frac{\partial}{\partial\sigma_w^2}\ln p(\mathbf{Y}|\mathcal{H}_1) = -\frac{N}{2}\sum_{i=1}^{M}\frac{1}{(E_s\sigma_h^2\alpha_i+\sigma_w^2)} + \sum_{k=0}^{N-1}\sum_{i=1}^{M}\frac{y_i^2[k]}{(E_s\sigma_h^2\alpha_i+\sigma_w^2)^2} \approx \frac{1}{\sigma_w^4}\left[\sum_{i=1}^{M}\frac{N}{2}\big(E_s\sigma_h^2\alpha_i+\sigma_w^2\big) - \sum_{k=0}^{N-1}\sum_{i=1}^{M}y_i^2[k]\right]=0. \tag{111}$$

We can use the following approximation

$$E_s\sigma_h^2\alpha_i+\sigma_w^2\approx\sigma_w^2 \tag{112}$$

in (111) since $E_s\sigma_h^2\alpha_i \ll \sigma_w^2$ in the case of the weak PU signal, i.e., the low SNR by initial conditions. We can simplify and rewrite (111) in the following form:

$$\frac{NE_s\sigma_h^2}{2}\sum_{i=1}^{M}\alpha_i + \frac{NM}{2}\sigma_w^2 - N\sum_{i=1}^{M}\lambda_{R_xi}=0. \tag{113}$$

Solving (113) with respect to σ_w^2 we can define the MLE $\hat{\sigma}_1^2$ under the hypothesis $\mathcal{H}_1$:

$$\hat{\sigma}_1^2 = \frac{2}{M}\sum_{i=1}^{M}\lambda_{R_xi} - \frac{E_s\sigma_h^2}{M}\sum_{i=1}^{M}\alpha_i. \tag{114}$$

Appendix 2

We say that the random variable x has a chi-square χ^2 distribution with υ degree of freedom if its probability density function (pdf) is determined as

$$p(x) = cx^{0.5\upsilon-1}\exp(-0.5x), \tag{115}$$

where c is a constant given by [50]

$$c=\frac{1}{2^{0.5\upsilon}\Gamma(0.5\upsilon)}, \tag{116}$$

$\Gamma(\cdot)$ is the gamma function. The MGF general form for the chi-square χ^2 distributed random variable x is given by [33]

$$\mathcal{M}_x(l) = E\big[\exp(lx)\big] = \int_{-\infty}^{\infty}\exp(lx)p(x)dx = c\int_0^{\infty}\exp(lx)x^{0.5\upsilon-1}\exp(-0.5x)dx. \tag{117}$$

At $\upsilon=1$, the constant c can be presented in the following form:

$$c=\frac{1}{2^{0.5\upsilon}\Gamma(0.5\upsilon)}=\frac{1}{\sqrt{2\pi}}. \tag{118}$$

Assume that $z_{1_i}[k]=\zeta_i^2$ and $z_{2_i}[k]=\eta_i^2$. The pdf for the random variables $z_{1_i}[k]$ and $z_{2_i}[k]$ are defined by the chi-square χ^2 distribution law with one degree of freedom [22]:

$$p(z_{1_i}) = \frac{1}{\sqrt{2\pi z_{1_i}\sigma_w^2}}\exp\left\{-\frac{z_{1_i}}{2\sigma_w^2}\right\}, \quad z_{1_i}>0, \tag{119}$$

$$p(z_{2_i}) = \frac{1}{\sqrt{2\pi z_{2_i}\sigma_w^2}}\exp\left\{-\frac{z_{2_i}}{2\sigma_w^2}\right\}, \quad z_{2_i}>0. \tag{120}$$

Introduce a new variable $z_i = z_{1_i}-z_{2_i}$. The MGF of the random variable z_i is given using the following formula:

$$\mathcal{M}_{z_i}(l) = E\big[\exp(lz_i)\big] = E\big\{\exp\big[l(z_{1_i}-z_{2_i})\big]\big\} = E\big[\exp(lz_{1_i})\exp(-lz_{2_i})\big] = E\big[\exp(lz_{1_i})\big]E\big[\exp(-lz_{2_i})\big] = \mathcal{M}_{z_{1_i}}(l)\mathcal{M}_{z_{2_i}}(-l). \tag{121}$$

The MGF of the random variable z_{1_i} is defined in the following form:

$$\mathcal{M}_{z_{1_i}}(l) = \frac{1}{\sqrt{2\pi\sigma_w^2}}\int_0^{\infty}\exp(lz_{1_i})z_{1_i}^{-0.5}\exp\left\{-\frac{z_{1_i}}{2\sigma_w^2}\right\}dz_{1_i} = \frac{1}{\sqrt{2\pi\sigma_w^2}}\int_0^{\infty}z_{1_i}^{-0.5}\exp\left\{-\left[\frac{1}{2\sigma_w^2}-l\right]z_{1_i}\right\}dz_{1_i}. \tag{122}$$

Introducing the variable $g_i=(0.5\sigma_w^{-2}-l)z_{1_i}$, after some mathematical transformations we can write

$$\mathcal{M}_{z_{1_i}}(l) = \frac{1}{\sqrt{\pi(1-2\sigma_w^2 l)}}\int_0^{\infty}g^{-0.5}\exp(-g_i)dg_i. \tag{123}$$

Based on definition of the gamma function [51]

$$\Gamma(x)=\int_0^{\infty}l^{x-1}\exp(-l)dl, \tag{124}$$

we obtain

$$\int_0^{\infty}g_i^{-0.5}\exp(-g_i)dg_i=\Gamma(0.5)=\sqrt{\pi}. \tag{125}$$

Finally, the MGF of the random variable z_{1_i} is defined as

$$\mathcal{M}_{z_{1_i}}(l) = \frac{\sqrt{\pi}}{\sqrt{\pi(1-2\sigma_w^2 l)}} = \frac{1}{\sqrt{1-2\sigma_w^2 l}}. \tag{126}$$

The mean and variance of the random variable z_{1_i} can be determined in the following form:

$$E[z_{1_i}] = \left.\frac{\partial\mathcal{M}_{z_{1_i}}(l)}{\partial l}\right|_{l=0} = \sigma_w^2, \tag{127}$$

$$Var[z_{1_i}] = E\big[z_{1_i}^2\big] - E[z_{1_i}]^2 = \left.\frac{\partial^2\mathcal{M}_{z_{1_i}}(l)}{\partial^2 l}\right|_{l=0} - E[z_{1_i}]^2 = 3\sigma_w^4-\sigma_w^4 = 2\sigma_w^4. \tag{128}$$

By the analogous way, we can find that the MGF of the random variable z_{1_i} takes the following form:

$$\mathcal{M}_{z_{2_i}}(-l) = \frac{1}{\sqrt{1+2\sigma_w^2 l}}. \tag{129}$$

Since $\{s_i[k]\}_{i=1}^{M}$ are spatially correlated for the i-th antenna array elements, the MGF of $\sum_{i=1}^{M} s_i^2[k]$ is defined as

$$\mathcal{M}_{\sum_{i=1}^{M} s_i^2[k]}(l) = \prod_{i=1}^{M}\left[1 - E_s\sigma_h^2\alpha_i l\right]^{-1}, \tag{130}$$

where α_i is the eigenvalue of the i-th spatial channel of the correlation matrix $\mathbf{R}$ given by (2). Based on (126), (129), and (130), the MGF of the GD partial decision statistics $T_{GD}(\mathbf{X}_k)$ is determined in the following form:

$$\begin{aligned}
&\mathcal{M}_{T_{GD}(\mathbf{X}_k)}(l)\\
&= \prod_{i=1}^{M}\left[1 - E_s\sigma_h^2\alpha_i l\right]^{-1}\prod_{i=1}^{M}\mathcal{M}_{z_{1_i}}(l)\prod_{i=1}^{M}\mathcal{M}_{z_{2_i}}(-l)\\
&= \prod_{i=1}^{M}\left[1 - E_s\sigma_h^2\alpha_i l\right]^{-1}\prod_{i=1}^{M}\left(1 - 2\sigma_w^2 l\right)^{-0.5}\prod_{i=1}^{M}\left(1 + 2\sigma_w^2 l\right)^{-0.5}\\
&= \prod_{i=1}^{M}\left[1 - E_s\sigma_h^2\alpha_i l\right]^{-1}\left(1 - 2\sigma_w^2 l\right)^{-0.5M}\left(1 + 2\sigma_w^2 l\right)^{-0.5M}\\
&= \left(1 - 4\sigma_w^4 l^2\right)^{-0.5M}\prod_{i=1}^{M}\left[1 - E_s\sigma_h^2\alpha_i l\right]^{-1}.
\end{aligned} \tag{131}$$

Appendix 3

The case 1: $\mu = 1$, $\beta = 1$. We can rewrite (59) as

$$\begin{aligned}
&\frac{1}{2\sqrt{2\pi NM(E_s^2\sigma_h^4 + 4\sigma_w^4)}}\exp\left\{-\frac{[THR_{GD} - NME_s\sigma_h^2]^2}{2NM(E_s^2\sigma_h^4 + 4\sigma_w^4)}\right\}\\
&- \frac{1}{4\sqrt{2\pi NM\sigma_w^4}}\exp\left\{-\frac{THR_{GD}^2}{8NM\sigma_w^4}\right\} = 0
\end{aligned} \tag{132}$$

or

$$\begin{aligned}
&\frac{1}{\sqrt{E_s^2\sigma_h^4 + 4\sigma_w^4}}\exp\left\{-\frac{[THR_{GD} - NME_s\sigma_h^2]^2}{2NM(E_s^2\sigma_h^4 + 4\sigma_w^4)}\right\}\\
&- \frac{1}{2\sigma_w^2}\exp\left\{-\frac{THR_{GD}^2}{8NM\sigma_w^4}\right\} = 0.
\end{aligned} \tag{133}$$

We can rewrite (133) in the following form

$$\frac{\exp\{-\frac{[THR_{GD} - NME_s\sigma_h^2]^2}{2NM(E_s^2\sigma_h^4 + 4\sigma_w^4)}\}}{\exp\{-\frac{THR_{GD}^2}{8NM\sigma_w^4}\}} = \frac{\sqrt{E_s^2\sigma_h^4 + 4\sigma_w^4}}{2\sigma_w^2} \tag{134}$$

or as

$$\exp\left\{-\frac{[THR_{GD} - NME_s\sigma_h^2]^2}{2NM(E_s^2\sigma_h^4 + 4\sigma_w^4)} + \frac{THR_{GD}^2}{8NM\sigma_w^4}\right\} = \frac{\sqrt{E_s^2\sigma_h^4 + 4\sigma_w^4}}{2\sigma_w^2}. \tag{135}$$

Taking the natural logarithm, we obtain

$$-\frac{[THR_{GD} - NME_s\sigma_h^2]^2}{2NM(E_s^2\sigma_h^4 + 4\sigma_w^4)} + \frac{THR_{GD}^2}{8NM\sigma_w^4} = \ln\frac{\sqrt{E_s^2\sigma_h^4 + 4\sigma_w^4}}{2\sigma_w^2}. \tag{136}$$

Taking into consideration that SNR in cognitive radio networks is very small, $\gamma \ll 1$ we can think $\sqrt{E_s^2\sigma_h^4 + 4\sigma_w^4}/2\sigma_w^2 \to 1$ and $\ln[\sqrt{E_s^2\sigma_h^4 + 4\sigma_w^4}/2\sigma_w^2] \to 0$. After some mathematical transformations we obtain

$$E_s^2\sigma_h^4 \times THR_{GD}^2 + 8NME_s^2\sigma_h^4\sigma_w^4 \times THR_{GD} - 4N^2M^2E_s^2\sigma_h^4\sigma_w^4 = 0. \tag{137}$$

Solution of the quadratic equation (137) is well-known and takes the form:

$$THR_{GD}^{op} = \frac{-b \pm \sqrt{b^2 - 4ac}}{2a}, \tag{138}$$

where

$$a = E_s^2\sigma_h^4; \quad b = 8NME_s^2\sigma_h^4\sigma_w^4; \quad c = -4N^2M^2E_s^2\sigma_h^4\sigma_w^4. \tag{139}$$

Thus, the optimal threshold (138) takes a very simple form:

$$THR_{GD_{AWGN}}^{op} \approx 2NM\sigma_w^2. \tag{140}$$

The case 2: $\mu = 1$, $\beta \neq 1$. If the noise power at the GD AF and GD PF outputs is differed the GD optimal threshold THR_{GD}^{op} can be derived using the factor of proportionality β in the following form:

$$\begin{aligned}
THR_{GD}^{op} = \arg\min_{THR_{GD}}\frac{1}{2}\Bigg\{1 - \frac{1}{2}\operatorname{erfc}\Bigg\{\frac{[THR_{GD} - NME_s\sigma_h^2]^2}{\sqrt{2NM[E_s^2\sigma_h^4 + 2\sigma_w^4(1+\beta^2)]}}\Bigg\}\\
+ \frac{1}{2}\operatorname{erfc}\left\{\frac{THR_{GD}}{2\sigma_w^2\sqrt{NM(1+\beta^2)}}\right\}\Bigg\}.
\end{aligned} \tag{141}$$

Using (57) we obtain the following result

$$\begin{aligned}
&\frac{\partial[P_{error}^{GD}(THR_{GD})]}{\partial(THR_{GD})}\\
&= \frac{1}{2}\Bigg\{\frac{1}{\sqrt{2\pi NM[E_s^2\sigma_h^4 + 2\sigma_w^4(1+\beta^2)]}}\\
&\quad\times\exp\left\{-\frac{[THR_{GD} - NME_s\sigma_h^2]^2}{2NM[E_s^2\sigma_h^4 + 2\sigma_w^4(1+\beta^2)]}\right\}\\
&\quad- \frac{1}{2\sqrt{\pi NM\sigma_w^4(1+\beta^2)}}\exp\left\{-\frac{THR_{GD}^2}{4NM\sigma_w^4(1+\beta^2)}\right\}\Bigg\} = 0.
\end{aligned} \tag{142}$$

We can rewrite (142) as

$$\begin{aligned}
&\frac{1}{\sqrt{2\pi NM[E_s^2\sigma_h^4 + 2\sigma_w^4(1+\beta^2)]}}\\
&\quad\times\exp\left\{-\frac{[THR_{GD} - NME_s\sigma_h^2]^2}{2NM[E_s^2\sigma_h^4 + 2\sigma_w^4(1+\beta^2)]}\right\}\\
&= -\frac{1}{2\sqrt{\pi NM\sigma_w^4(1+\beta^2)}}\exp\left\{-\frac{THR_{GD}^2}{4NM\sigma_w^4(1+\beta^2)}\right\}
\end{aligned}$$

or

$$\frac{\exp\{-\frac{[THR_{GD} - NME_s\sigma_h^2]^2}{2NM[E_s^2\sigma_h^4 + 2\sigma_w^4(1+\beta^2)]}\}}{\exp\{-\frac{THR_{GD}^2}{4NM\sigma_w^4(1+\beta^2)}\}} = \sqrt{\frac{2[E_s^2\sigma_h^4 + 2\sigma_w^4(1+\beta^2)]}{4\sigma_w^4(1+\beta^2)}}$$

or

$$\begin{aligned}
&\exp\left\{-\frac{[THR_{GD} - NME_s\sigma_h^2]^2}{2NM[E_s^2\sigma_h^4 + 2\sigma_w^4(1+\beta^2)]} + \frac{THR_{GD}^2}{4NM\sigma_w^4(1+\beta^2)}\right\}\\
&= \sqrt{\frac{2[E_s^2\sigma_h^4 + 2\sigma_w^4(1+\beta^2)]}{4\sigma_w^4(1+\beta^2)}}.
\end{aligned} \tag{143}$$

Taking the natural logarithm, we obtain

$$-\frac{[THR_{GD}-NME_s\sigma_h^2]^2}{2NM[E_s^2\sigma_h^4+2\sigma_w^4(1+\beta^2)]}+\frac{THR_{GD}^2}{4NM\sigma_w^4(1+\beta^2)}=\ln\sqrt{\frac{2[E_s^2\sigma_h^4+2\sigma_w^4(1+\beta^2)]}{4\sigma_w^4(1+\beta^2)}}. \quad (144)$$

Taking into consideration that SNR in cognitive radio networks is very small, $\gamma \ll 1$ we can think $\sqrt{E_s^2\sigma_h^4+4\sigma_w^4}/2\sigma_w^2 \to 1$ and $\ln[\sqrt{E_s^2\sigma_h^4+4\sigma_w^4}/2\sigma_w^2] \to 0$. After some mathematical transformations we obtain

$$E_s^2\sigma_h^4\times THR_{GD}^2+8NME_s^2\sigma_h^4\sigma_w^4(1+\beta^2)\times THR_{GD}-2N^2M^2E_s^2\sigma_h^4\sigma_w^4(1+\beta^2)=0. \quad (145)$$

Solution of the quadratic equation (145) is well-known where

$$a=E_s^2\sigma_h^4;\quad b=8NME_s^2\sigma_h^4\sigma_w^4(1+\beta^2);\quad c=2N^2M^2E_s^2\sigma_h^4\sigma_w^4(1+\beta^2). \quad (146)$$

Substituting (146) into (138) we obtain

$$THR_{GD_{AWGN}}^{op}=NM\sigma_w^2\sqrt{2(1+\beta^2)}. \quad (147)$$

The case 3: $\mu \neq 1$, $\beta = 1$. Equation (88) can be simplified and we obtain

$$\exp\left\{-\frac{[THR_{GD}-NM(2\mu-1)E_s\sigma_h^2]^2}{NM[(2\mu-1)^2E_s^2\sigma_h^4+4(\mu-1)^2E_s\sigma_h^2+4\sigma_w^4]}+\frac{THR_{GD}^2}{8NM\sigma_w^4}\right\}=\frac{1}{2\sigma_w^2}\sqrt{(2\mu-1)^2E_s^2\sigma_h^4+4(\mu-1)^2E_s\sigma_h^2+4\sigma_w^4}. \quad (148)$$

Taking the natural logarithm of (150), we have

$$-\frac{[THR_{GD}-NM(2\mu-1)E_s\sigma_h^2]^2}{NM[(2\mu-1)^2E_s^2\sigma_h^4+4(\mu-1)^2E_s\sigma_h^2+4\sigma_w^4]}+\frac{THR_{GD}^2}{8NM\sigma_w^4}=\ln\frac{1}{2\sigma_w^2}\sqrt{(2\mu-1)^2E_s^2\sigma_h^4+4(\mu-1)^2E_s\sigma_h^2+4\sigma_w^4}. \quad (149)$$

Following the same previous steps and applying the approximation of low SNR, $\gamma \ll 1$ and after some mathematical transformations we obtain

$$[(2\mu-1)^2E_s^2\sigma_h^4+4(\mu-1)^2E_s\sigma_h^2+4\sigma_w^4]\times THR_{GD}^2+16NME_s\sigma_h^2\sigma_w^4(2\mu-1)\times THR_{GD}-8N^2M^2E_s^2\sigma_h^4\sigma_w^4(2\mu-1)^2=0. \quad (150)$$

Solving (150) will give us the required optimal GD threshold

$$THR_{GD_{AWGN}}^{op}\approx 2(2\mu-1)NM\sigma_w^2. \quad (151)$$

The case 4: $\mu \neq 1$, $\beta \neq 1$. Equation (65) can be simplified and we obtain

$$\exp\left\{-\frac{[THR_{GD}-NM(2\mu-1)E_s\sigma_h^2]^2}{2NM[(2\mu-1)^2E_s^2\sigma_h^4+2(\mu-1)^2E_s\sigma_h^2(1+\beta)+2\sigma_w^4(1+\beta^2)]}+\frac{THR_{GD}^2}{4NM\sigma_w^4(1+\beta^2)}\right\}=\frac{1}{2\sigma_w^2}\sqrt{(2\mu-1)^2E_s^2\sigma_h^4+2(\mu-1)^2E_s\sigma_h^2(1+\beta)+2\sigma_w^4(1+\beta^2)}. \quad (152)$$

Applying the same steps and after some mathematical transformations we obtain the following quadratic equation:

$$(\mu-1)^2E_s\sigma_h^2(1+\beta)\times THR_{GD}^2+2NM(2\mu-1)E_s\sigma_h^2\sigma_w^4(1+\beta^2)\times THR_{GD}-N^2M^2E_s^2\sigma_h^2\sigma_w^4(2\mu-1)(1+\beta^2)=0. \quad (153)$$

By solving (153) we can present the GD optimal threshold for this case using the following form:

$$THR_{GD_{AWGN}}^{op}\approx\frac{2NM(2\mu-1)(1+\beta^2)}{(\mu-1)^2(1+\beta)}. \quad (154)$$

The normalized GD optimal threshold with the normalization factor NM is determined in the following form:

$$\mathcal{THR}_{GD_{AWGN}}^{op}\approx\frac{THR_{GD_{AWGN}}^{op}}{NM}=\frac{2(2\mu-1)(1+\beta^2)}{(\mu-1)^2(1+\beta)}. \quad (155)$$

References

[1] S. Sharma, T. Bogale, S. Chatzinotas, B. Ottersten, L. Le, X. Wang, Cognitive radio techniques under practical imperfections: a survey, IEEE Commun. Surv. Tutor. 17 (4) (July 2015) 1858–1884, https://doi.org/10.1109/COMST.2015.2452414.

[2] J. Song, Z. Feng, P. Zhang, Z. Liu, Spectrum sensing in cognitive radios based on enhanced energy detector, IET Commun. 6 (8) (May 2012) 805–809.

[3] S.M. Kay, Fundamentals of Statistical Signal Processing: Detection Theory, vol. 2, Prentice Hall, New Jersey, USA, 1998.

[4] T.J. Lim, R. Zhang, Y.C. Liang, Y. Zeng, GLRT-based spectrum sensing for cognitive radio, in: Proc. IEEE Global Telecommunications Conference, GLOBECOM 2008, New Orleans, LA, USA, 2008, pp. 1–5.

[5] H.S. Chen, W. Gao, D.G. Daut, Signature based spectrum sensing algorithms for IEEE 802.22 WRAN, in: Proceedings of IEEE International Conference on Communications, ICC, Glasgow, Scotland, 2007, pp. 6487–6492.

[6] Q. Lv, F. Gao, Matched filter based spectrum sensing and power level recognition with multiple antennas, in: Proceedings of IEEE China Summit and International Conference on Signal and Information Processing, ChinaSIP, Chengdu, China, 2015, pp. 305–309.

[7] W.M. Jang, Blind cyclostationary spectrum sensing in cognitive radios, IEEE Commun. Lett. 18 (3) (March 2014) 393–396.

[8] P. Urriza, E. Rebeiz, D. Cabric, Multiple antenna cyclostationary spectrum sensing based on the cyclic correlation significance test, IEEE J. Sel. Areas Commun. 31 (11) (2013) 2185–2195.

[9] A. Kortun, T. Ratnarajah, M. Sellathurai, Y. Liang, Y. Zeng, On the eigenvalue-based spectrum sensing and secondary user throughput, IEEE Trans. Veh. Technol. 63 (3) (2014) 1480–1486.

[10] M. Jin, Y. Li, H.-G. Ryu, On the performance of covariance based spectrum sensing for cognitive radio, IEEE Trans. Signal Process. 60 (7) (July 2012) 3670–3682.

[11] Y. Zeng, Y.C. Liang, Maximum-minimum eigenvalue detection for cognitive radio, in: Proceedings of IEEE 18th International. Symposium on Personal, Indoor and Mobile Radio Communications, PIMRC'07, Athens, Greece, 2007, pp. 1–5.

[12] Y. Zeng, Y.-C. Liang, Eigenvalue-based spectrum sensing algorithms for cognitive radio, IEEE Trans. Commun. 57 (6) (June 2009) 1784–1793.

[13] P. Wang, et al., Multiantenna-assisted spectrum sensing for cognitive radio, IEEE Trans. Veh. Technol. 59 (4) (May 2010) 1791–1800.

[14] T. Bogale, L. Vandendorpe, L.B. Le, Wideband sensing and optimization for cognitive radio networks with noise variance uncertainty, IEEE Trans. Commun. 63 (4) (April 2015) 1091–1105.

[15] T. Bogale, L. Vandendorpe, Max-min SNR signal energy based spectrum sensing algorithms for cognitive radio net-works with noise variance uncertainty, IEEE Trans. Wirel. Commun. 30 (1) (Jan. 2014) 280–290.

[16] A. Mariani, A. Giorgetti, M. Chiani, Effects of noise power estimation on energy detection for cognitive radio applications, IEEE Trans. Commun. 59 (12) (Dec. 2011) 3410–3420.

[17] G. Yu, C. Long, M. Xiang, W. Xi, A novel energy detection scheme based on dynamic threshold in cognitive radio systems, J. Comput. Inf. Syst. 8 (6) (2012) 2245–2252.

[18] P. Mane, S. Nikam, Spectrum sensing in cognitive radio using TSA, Int. J. Comput. Netw. Wirel. Commun. 2 (4) (Aug. 2012) 514–518.

[19] H. Chen, J. Liu, Cooperative spectrum sensing based on double threshold detection and Dempster-Shafer theory, in: Proceedings of 12th IEEE International Conference on Communication Technology, ICCT, Nanjing, China, 2010, pp. 1212–1215.

[20] L. Luo, P. Zhang, G. Zhang, J. Qin, Spectrum sensing for cognitive radio networks with correlated multiple antennas, Electron. Lett. 47 (23) (Nov. 2011) 1297–1298.

[21] V. Tuzlukov, A new approach to signal detection theory, Digit. Signal Process. 8 (3) (1998) 166–184.

[22] V. Tuzlukov, Signal Detection Theory, Springer-Verlag, Boston, USA, 2001, 725 pp.
[23] V. Tuzlukov, Signal Processing Noise, CRC Press, Taylor & Francis Group, Boca Raton, London, New York, Washington D.C., USA, 2002, 663 pp.
[24] V. Tuzlukov, Generalized approach to signal processing in wireless communications: the main aspects and some examples, in: A. Eksim (Ed.), Wireless Communications and Networks: Recent Advances, InTech, Rijeka, Croatia, 2012, pp. 305–338, Chapter 11.
[25] V. Tuzlukov, DS-CDMA downlink systems with fading channel employing the generalized receiver, Digit. Signal Process. 21 (6) (2011) 725–733.
[26] V. Tuzlukov, Signal processing by generalized receiver in DS-CDMA wireless communication systems with frequency-selective channels, Circuits Syst. Signal Process. 30 (6) (2011) 1197–1230.
[27] V. Tuzlukov, Signal processing by generalized receiver in DS-CDMA wireless communication systems with optimal combining and partial cancellation, EURASIP J. Adv. Signal Process. 2011 (2011) 913189, https://doi.org/10.1155/2011/913189, 15 pages.
[28] V. Tuzlukov, Bit error probability of quadriphase DS-CDMA wireless communication systems based on generalized approach to signal processing, Telecommun. Rev. 23 (4) (2013) 501–515.
[29] V. Tuzlukov (Ed.), Communication Systems: New Research, NOVA Science Publishers, Inc., New York, USA, 2013, 423 pp.
[30] V. Tuzlukov, Wireless communications: generalized approach to signal processing, in: Communication Systems: New Research, NOVA Science Publishers, Inc., New York, USA, 2013, pp. 175–268, Chapter 6.
[31] V. Tuzlukov, Error probability performance of quadriphase DS-CDMA wireless communication systems based on generalized approach to signal processing, WSEAS Trans. Commun. 13 (2) (2014) 116–129.
[32] V. Tuzlukov, Signal Processing in Radar System, Taylor & Francis Group, CRC Press, Boca Raton, London, New York, Washington D.C., 2012, 632 pp.
[33] M. Shbat, V. Tuzlukov, Noise power estimation under generalized detector employment in automotive detection and tracking systems, in: Proceedings 9th IET Data Fusion and Target Tracking Conference, DF&TT'12, London, UK, May 16–17, 2012.
[34] V. Tuzlukov, Implementation of generalized detector in MIMO radar systems, WSEAS Trans. Commun. 12 (3) (2013) 107–120.
[35] M. Shbat, V. Tuzlukov, Evaluation of detection performance under employment of the generalized detector in radar sensor systems, Radioengineering 23 (1) (2014) 50–65.
[36] M. Shbat, V. Tuzlukov, Definition of adaptive detection threshold under employment of the generalized detector in radar sensor systems, IET Signal Process. 8 (6) (2014) 622–632.
[37] V. Tuzlukov, Adaptive detection of range-spread targets in Gaussian noise using the generalized detector, WSEAS Trans. Commun. 13 (2014) 606–621 (paper #67).
[38] V. Tuzlukov, Parametric Rao test for multichannel adaptive generalized detector, WSEAS Trans. Signal Process. 10 (2014) 561–575 (paper #58).
[39] M. Shbat, Performance Analysis of Signal Detection by GD in Radar Sensor and Cognitive Radio Systems, PhD Thesis, Kyungpook National University, 2014.
[40] M. Shbat, V. Tuzlukov, Spectrum sensing under correlated antenna array using generalized detector in cognitive radio systems, Int. J. Antennas Propag. 2013 (2013) 853746, https://doi.org/10.1155/2013/853746 (8 pages).
[41] M. Shbat, V. Tuzlukov, SNR wall phenomenon alleviation using generalized detector for spectrum sensing in cognitive radio networks, Sensors 5 (7) (July 2015) 16105–16135.
[42] S. Kim, J. Lee, H. Wang, D. Hong, Sensing performance of energy detector with correlated multiple antennas, IEEE Signal Process. Lett. 16 (8) (2009) 671–674.
[43] M. Jin, Y. Li, Z. Zhang, R. Wang, A new spectrum sensing algorithm based on antenna correlation for cognitive radio systems, Wirel. Pers. Commun. 66 (2012) 419–428, https://doi.org/10.1007/s11277-011-0349-9.
[44] A. Molisch, L. Greenstein, M. Shafi, Propagation issues for cognitive radio, Proc. IEEE 97 (5) (May 2009) 787–804.
[45] S. Loyka, Channel capacity of MIMO architecture using the exponential correlation matrix, IEEE Commun. Lett. (5) (2001) 369–371.
[46] G. Durgin, T. Rappaport, Effects of multipath angular spread on the spatial cross-correlation of received voltage envelopes, in: Proceedings IEEE 49th Vehicular Technology Conference, vol. 2, Houston, Texas, USA, 1999, pp. 996–1000.
[47] M. Maximov, Joint correlation of fluctuative noise at outputs of frequency filters, Radioengineering 9 (1956) 28–38.
[48] Y. Chernyak, Joint correlation of noise voltage at outputs of amplifiers with nonoverlapping responses, Radio Phys. Electron. (4) (1960) 551–561.
[49] M. Simon, M. Alouini, Digital Communication over Fading Channels, 2nd edn., Wiley, New York, 2005.
[50] D. Gradshteyn, I. Ryzhik, Table of Integrals, Series, and Product, 7th edn., Academic Press, Amsterdam, Boston, London, New York, Oxford, Paris, San Diego, San Francisco, Singapore, Sydney, Tokyo, Boca Raton, London, New York, Washington D.C., 2007.
[51] A. Prudnikov, Y. Brychkov, O. Marichev, Integrals and Series, vol. 2, Gordon & Breach Science Publishers, 1986.
[52] N. Beaulieu, C. Cheng, Efficient Nakagami-*m* fading channel simulation, IEEE Trans. Veh. Technol. 54 (2) (2005) 413–424.
[53] S. Kate, S. Navare, S. Bandewar, C. Lande, A. Tambe, R. Acharya, V. Pawar, S. Gaikwad, Engineering Mathematics – II, Technical Publications, Pune, India, 2007.
[54] IEEE 802.22 Working Group on Wireless Regional Area Networks (WRAN), http://grouper.ieee.org/groups/802/22/.
[55] R. Tandra, A. Sahai, *SNR* walls for signal detection, IEEE J. Sel. Top. Signal Process. 2 (1) (2008) 4–17.
[56] S. Atapattu, C. Tellambura, H. Jiang, Spectrum sensing via energy detector in low *SNR*, in: Proceedings IEEE International Conference on Communications, ICC 2011, Kyoto, Japan, 2011, pp. 1–5.

Modar Shbat graduated from Damascus University, Faculty of Mechanical and Electrical Engineering as an electronics engineer in 2003. In 2005, he got a post graduate diploma in telecommunications engineering from Damascus University. He received master degree (M.Sc) in information and communications engineering from Korea Advanced Institute of Science and Technology (KAIST)/South Korea in 2008. He obtained his PhD degree in electronics engineering from Kyungpook National University (KNU), South Korea (Signal Processing Lab) in February 2014. Currently, Dr. Modar works for Polytechnic University of San Luis Potosi (Mexico) as an Assistant Professor in Networks and Telecommunications Engineering (IRTEL) Department. His research interests include: signal detection and processing algorithms, spectrum sensing in cognitive radio, smart antennas and beam-forming algorithms, and others. Dr. Modar Shbat scientific work and research accomplishments are published in peer reviewed journals, books, and presented in international conferences.

Vyacheslav Tuzlukov received the MSc and PhD degrees in radio physics from the Belorussian State University, Minsk, Belarus in 1976 and 1990, respectively, and DSc degree from the Kotelnikov Institute of Radioengineering and Electronics of Russian Academy of Sciences in 1995. From 2000 to 2002 he was a Visiting Professor at the University of Aizu, Japan and from 2003 to 2007 served as an Invited Professor at the Ajou University, Suwon, South Korea, within the Department of Electrical and Computer Engineering. Since March 2008 to February 2009 he joined as Full Professor at the Yeungnam University, Gyeonsang, South Korea within the School of Electronic Engineering, Communication Engineering, and Computer Science. Starting from March 2009 to March 2016 he served as a Full Professor and Director of Signal Processing Lab at the Department of Communication and Information Technologies, School of Electronics Engineering, College of IT Engineering, Kyungpook National University, Daegu, South Korea. He joined to Belarussian State Air Force Academy in September 2016 and served as a Head of Department till February 2018. Currently he is a Full Professor of the Belarussian State Academy of Communications. His research emphasis is on signal processing in radar, wireless communications, wireless sensor networks, remote sensing, sonar, satellite communications, mobile communications, and other signal processing systems. He is the author over 260 journal and conference papers, seventeenth books in signal processing published by Springer-Verlag and CRC Press, some of them are *Signal Detection Theory* (2001), *Signal Processing Noise* (2002), *Signal and Image Processing in Navigational Systems* (2005), *Signal Processing in Radar Systems* (2012), Editor of the book *Communication Systems: New Research* (2013), Nova Science Publishers, Inc, USA, and has also contributed Chapters "Underwater Acoustical Signal Processing" and "Satellite Communications Systems: Applications" to *Electrical Engineering Handbook: 3rd Edition*, 2005, CRC Press; "Generalized Approach to Signal Processing in Wireless Communications: The Main Aspects and Some Examples" to *Wireless Communications and Networks: Recent Advances*, InTech, 2012; "Radar Sensor Detectors for Vehicle Safety Systems" to *Electrical and Hybrid Vehicles: Advanced Systems, Automotive Technologies, and Environmental and Social Implications*, Nova Science Publishers, Inc., USA, 2014; "Wireless Communications: Generalized Approach to Signal Processing" and "Radio Resource Management and Femtocell Employment in LTE Networks", to *Communication Systems: New Research*, Nova Science Publishers, Inc., USA, 2013, and "Radar Sensor Detectors for Vehicle Safety Systems" to *Autonomous Vehicles: Intelligent Transport Systems and Automotive Technologies*, Publishing House, University of Pitesti, Romania, 2013. He serves as a Chair of International Conferences on Signal Processing, Keynote Speaker, Plenary Lecturer, Chair of Sessions, Tutorial Instructor and organizes Special Sections at the major International Conferences and Symposia on signal processing. Dr. Tuzlukov is the Editor-in-Chief of the *SOP Transactions*

on Signal Processing journal and *American Journal of Sensor Technology*. Dr. Tuzlukov was highly recommended by U.S. experts of Defense Research and Engineering (DDR& E) of the United States Department of Defense as a recognized expert in the field of humanitarian demining and minefield sensing technologies and had been awarded by Special Prize of the United States Department of Defense in 1999. Dr. Tuzlukov is distinguished as one of the leading achievers from around the world by Marquis Who's Who and his name and biography have been included in the Who's Who in the World, 2006-2013; Who's Who in World, 25th Silver Anniversary Edition, 2008, Marquis Publisher, NJ, USA; Who's Who in Science and Engineering, 2006-2012 and Who's Who in Science and Engineering, 10th Anniversary Edition, 2008-2009, Marquis Publisher, NJ, USA; 2009-2010 Princeton Premier Business Leaders and Professionals Honors Edition, Princeton Premier Publisher, NY, USA; 2009 Strathmore's Who's Who Edition, Strathmore's Who's Who Publisher, NY, USA; 2009 Presidental Who's Who Edition, Presidental Who's Who Publisher, NY, USA; Who's Who among Executives and Professionals, 2010 Edition, Marquis Publisher, NJ, USA; Who's Who in Asia 2012, 2nd Edition, Marquis Publisher, NJ, USA; Top 100 Executives of 2013 Magazine, Super Network Publisher, New York, USA, 2013; 2013/2014 Edition of the Global Professional Network, Business Network Publisher, New York, USA, 2013; 2013/2014 Edition of the Who's Who Network Online, Business Network Publisher, New York, USA, 2014; Online Professional Gateway, 2014 Edition, Business Network Publisher, New York, USA, 2014; 2014 "Worldwide Who's Who", Marquis Publisher, NJ, USA; "New 2014-Edition Executive Who's Who", Marquis Publisher, NJ, USA; 2014 Membership in the "Exclusive Top 100", USA; 2014 Strathmore Professional Biographies Edition, Strathmore's Who's Who Publisher, NY, USA; 2015 Who's Who of Executive and Professional Honors Edition, Marquis Publisher, NJ, USA; 2015 Worldwide Who's Who Membership, Marquis Publisher, NJ, USA; 2015-2016 Membership in the "Exclusive Top 100", USA.